

ARTICLE

Prolonged pharmacological inhibition of cathepsin C results in elimination of neutrophil serine proteases

Carla Guarino^{1,§}, Yveline Hamon^{1,6,§}, Cécile Croix^{2,§}, Anne-Sophie Lamort^{1,6}, Sandrine Dallet-Choisy¹, Sylvain Marchand-Adam¹, Adam Lesner³, Thomas Baranek¹, Marie-Claude Viaud-Massuard², Conni Lauritzen⁴, John Pedersen⁴, Nathalie Heuzé-Vourc'h¹, Mustapha Si-Tahar¹, Erhan Firatli⁵, Dieter E. Jenne⁶, Francis Gauthier¹, Marshall S. Horwitz^{7,#}, Niels Borregaard^{8,#} and Brice Korkmaz^{1,7*}

This work is dedicated to the memory of Prof. Niels Borregaard who died on 10th January 2017

§, # *Equal contribution*

¹INSERM U-1100, “Centre d’Etude des Pathologies Respiratoires” and Université François Rabelais, Tours, France; ²CNRS UMR-7292, “GICC, Innovation Moléculaire et Thérapeutique”, Université de Tours, 31 Avenue Monge, Tours, France; ³Faculty of Chemistry, University of Gdansk, Gdansk, Poland; ⁴Unizyme Laboratories A/S, Hørsholm, Denmark; ⁵Department of Periodontology, Faculty of Dentistry, University of Istanbul, Istanbul, Turkey; ⁶Comprehensive Pneumology Center, Institute of Lung Biology and Disease, German Center for Lung Research (DZL), Munich and Max Planck Institute of Neurobiology, Planegg-Martinsried, Germany; ⁷Department of Pathology, University of Washington, Seattle, WA, USA; ⁸The Granulocyte Research Laboratory, National University Hospital, Rigshospitalet, University of Copenhagen, Denmark

***Corresponding author:** Brice Korkmaz (PhD)

INSERM U-1100 “Centre d’Etude des Pathologies Respiratoires (CEPR)”,

Université François Rabelais, Faculté de Médecine

10 Bld. Tonnellé, 37032, Tours, France

e-mail: brice.korkmaz@inserm.fr

Tel: 0033 2 47 36 63 86

Fax: 0033 2 47 36 60 46

Abstract

Cathepsin C (CatC) is a tetrameric cysteine dipeptidyl aminopeptidase that plays a key role in activation of pro-inflammatory serine protease zymogens by removal of an N-terminal pro-dipeptide sequence. Loss of function mutations in the CatC gene are associated with lack of immune cell serine proteases activities and cause Papillon-Lefèvre syndrome (PLS). Also, only very low levels of elastase-like protease zymogens are detected by proteome analysis of neutrophils from PLS patients. Thus, CatC inhibitors represent new alternatives for the treatment of neutrophil protease-driven inflammatory or autoimmune diseases. We aimed to experimentally inactivate and lower neutrophil elastase-like proteases by pharmacological blocking of CatC-dependent maturation in cell-based assays and *in vivo*. Isolated, immature bone marrow cells from healthy donors pulse-chased in the presence of a new cell permeable cyclopropyl nitrile CatC inhibitor almost totally lack elastase. We confirmed the elimination of neutrophil elastase-like proteases by prolonged inhibition of CatC in a non-human primate. We also showed that neutrophils lacking elastase-like protease activities were still recruited to inflammatory sites. These preclinical results demonstrate that the disappearance of neutrophil elastase-like proteases as observed in PLS patients can be achieved by pharmacological inhibition of bone marrow CatC. Such a transitory inhibition of CatC might thus help to rebalance the protease load during chronic inflammatory diseases, which opens new perspectives for therapeutic applications in human.

Keywords: Cathepsin C, neutrophil, serine protease, cysteine protease, inhibitor, Papillon-Lefèvre syndrome

Abbreviations: ABP, activity-based probe; BALF, broncho-alveolar lavage fluid; Cat, cathepsin; FRET, fluorescence resonance energy transfer; GPA, granulomatosis with polyangiitis; HNE, human neutrophil elastase; HPLC, High Performance Liquid Chromatography; HRMS, high resolution mass spectrometry; LPS, lipopolysaccharide; MPO, myeloperoxidase; NGAL, neutrophil gelatinase-associated lipocalin; PR3, proteinase 3; PLS, Papillon-Lefèvre syndrome; hum, human; MF, *Macaca fascicularis*; WB, Western-blot.

ACCEPTED MANUSCRIPT

1. Introduction

Preclinical and clinical data suggest that inhibition of neutrophil serine proteases (elastase (HNE), proteinase 3 (PR3), cathepsin G (CatG)) using therapeutic inhibitors would suppress or attenuate deleterious effects of inflammatory disorders mediated by neutrophilic proteases such as COPD, cystic fibrosis, alpha-1-protease inhibitor deficiency¹. Likewise, broad spectrum inhibitors of neutrophil elastase-like proteases could achieve better protection of the lungs against noxious agents than highly selective monospecific small molecule inhibitors targeting individual neutrophilic proteases. Attempts to inhibit these proteases *in situ* still remain non-convincing due to the protective environment mucus and DNA in bronchial secretions, which compromise efficient inhibition of proteases by exogenous therapeutic inhibitors². Elimination of harmful elastase-like proteases would be also useful in granulomatosis with polyangiitis (GPA)³⁻⁵. GPA is a systemic vasculitis of small blood vessels and granulomatous inflammation of the upper and/or lower respiratory tracts characterized by a circulating autoantibody (ANCA)^{6, 7}. PR3 is identified as the prime antigenic target of ANCA in GPA⁸.

Dipeptidyl peptidase I (EC 3.4.14.1), also known as cathepsin C (CatC) is a highly conserved lysosomal cysteine dipeptidyl aminopeptidase belonging to the papain family^{9, 10}. The best characterized physiological function of CatC is the activation of pro-inflammatory granule-associated serine proteases, including neutrophil elastase-like proteases¹¹⁻¹³. These proteases are synthesized as inactive zymogen containing a N-terminal pro-dipeptide which maintains the zymogen in its inactive conformation and prevents premature activation potentially toxic to the cell¹⁴. The activation occurs through cleavage of the N-terminal dipeptide by CatC during neutrophil maturation in the bone marrow.

Loss of function mutations in the CatC gene (*CSTC*) are associated with Papillon-Lefèvre syndrome (PLS)^{15, 16}. PLS (MIM 245000) is a rare autosomal recessive disease characterized by severe periodontitis and hyperkeratosis of the hand, palms and foot soles^{17, 18}. The investigation of elastase-like proteases in neutrophils collected from PLS patients has demonstrated both reduced proteolytic activities and very low protein levels^{11, 13}. However, PLS patients do not exhibit marked immunodeficiency despite the absence of elastase-like proteases in circulating blood neutrophils¹⁹. Hence, transitory and/or partial inhibition of CatC in the precursor cells of the bone marrow represents an attractive therapeutic strategy to control the activity of serine proteases in chronic inflammatory lung diseases with a high neutrophil recruitment and to eliminate a pivotal antigen in GPA patients⁴.

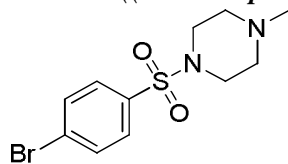
Several attempts have been made to inhibit CatC using a cell-permeable inhibitor²⁰⁻²². Near complete inhibition of elastase-like proteases has been achieved in human and murine immortalized hematopoietic cell lines^{23, 24}. However, the amounts of elastase-like zymogens were not lowered by pharmacological CatC inhibition, in contrast to what was observed in neutrophils from PLS patients^{23, 24}. Whether this was due to the use of immortalized cell lines, the protease content of which largely differs from that of bone marrow precursor cells, or to the fact that the disappearance of zymogens targeted by CatC was a consequence of the genetic inactivation of CatC observed in PLS²⁴ remains unanswered. In this work, we have investigated the fate of elastase-like zymogens in cultured human bone marrow promyelocytes from healthy donors in the presence of a new cell permeable potent nitrile CatC inhibitor (IcatC). Our results demonstrate that the disappearance of zymogens targeted by CatC is not a unique consequence of genetic inactivation of CatC. We then confirmed these results *in vivo* by long-term pharmacological targeting of CatC using IcatC, prior to induction of lung inflammation in *Macaca fascicularis* (*Mf*) and investigation of the recruitment of blood neutrophils into the lung airways.

2. Material and methods

2.1. Synthesis of IcatC

IcatC ((*S*)-2-amino-*N*-((1*R*,2*R*)-1-cyano-2-(4'-(4-methylpiperazin-1-ylsulfonyl)biphenyl-4-yl)cyclopropyl)butanamide) have been obtained in fourteen steps from the 4-bromobenzaldehyde and the Meldrum's acid (**Figure 1**). The 1-methyl-4-((4-(4,4,5,5-tetramethyl-1,3,2-dioxaborolan-2-yl)phenyl)sulfonyl)-piperazine have been also synthesized from 4-bromosulfonylchloride and *N*-methylpiperazine in moderate yield.

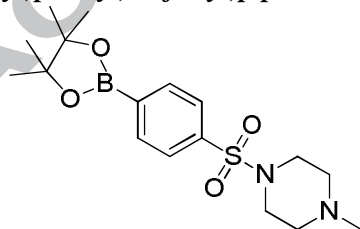
1-((4-Bromophenyl)sulfonyl)-4-methylpiperazine



To a solution of 4-bromobenzenesulfonylchloride (Fluorochem, UK) (6.00 g, 23.48 mmol) in tetrahydrofuran (40 mL) was added 1-methylpiperazine (Sigma-Aldrich, France) (3.9 mL, 35.22 mmol). The resulting reaction mixture was stirred at room temperature for 4 h. The solvent was removed and the residue was dissolved in dichloromethane (100 mL). The solution was washed with saturated aqueous sodium hydrogen carbonate (3 times), saturated aqueous sodium chloride, dried over magnesium sulfate and concentrated under reduced pressure to give 7.41 g (quantitative yield) of a white solid.

¹H NMR (300 MHz, CDCl₃) δ 7.70 - 7.64 (m, 2H), 7.64 - 7.56 (m, 2H), 3.10 - 2.95 (m, 4H), 2.59 - 2.38 (m, 4H), 2.26 (s, 3H).

1-Methyl-4-((4-(4,4,5,5-tetramethyl-1,3,2-dioxaborolan-2-yl)phenyl)sulfonyl)piperazine

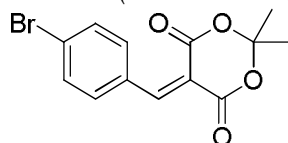


To a solution of 1-((4-bromophenyl)sulfonyl)-4-methylpiperazine (7.4 g, 23.20 mmol) in 1,4-dioxane (89 mL) and DMSO (7.4 mL) was added pinacolatodiboron (Fluorochem, UK) (17.67 g, 69.59 mmol), potassium acetate (Alfa Aesar, France) (4.56 g, 46.39 mmol) and PdCl₂(dppf) (Alfa Aesar, France) (849 mg, 1.16 mmol) under argon atmosphere. The mixture

was stirred at 100 °C for 16 h. After cooling, the reaction mixture was filtered. Most solvent was removed under reduce pressure and the residue was extracted with ethyl acetate. The organic layer was washed with saturated sodium chloride, dried over magnesium sulfate and concentrated under reduce pressure. The crude product was purified by flash column chromatography using a 95/5 v/v dichloromethane/methanol to afford 4.24 g (50 % yield) as a solid.

$^1\text{H NMR}$ (300 MHz, CDCl_3) δ 7.94 (d, $J = 8.3$ Hz, 2H), 7.72 (d, $J = 8.3$ Hz, 2H), 3.03 (s, 4H), 2.47 (s, 4H), 2.26 (s, 3H), 1.35 (s, 12H).

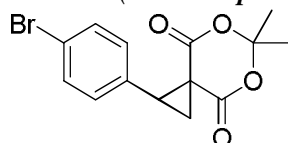
5-(4-Bromobenzylidene)-2,2-dimethyl-1,3-dioxane-4,6-dione



To a 1 L three-neck flask was added 4-bromobenzaldehyde (Fluorochem, UK) (20 g, 108.11 mmol) and Meldrum's acid (Fluorochem, UK) (17.12 g, 118.90 mmol). 220 mL of water was added and the mixture was stirred at 75 °C via mechanical stirrer for 3 h. Then the system was transferred to ice-bath and stayed overnight. The white solid was isolated by filtration and washed with 250 mL of water. The crude product was recrystallized from ethyl acetate and ethanol to afford 13.78 g (41% yield) of a white solid.

$^1\text{H NMR}$ (300 MHz, DMSO) δ 8.34 (s, 1H), 7.96 - 7.91 (m, 2H), 7.76 - 7.69 (m, 2H), 1.76 (s, 6H).

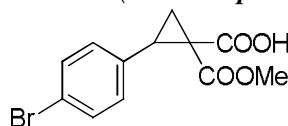
1-(4-Bromophenyl)-6,6-dimethyl-5,7-dioxaspiro[2.5]octane-4,8-dione



To a cooled solution of 5-(4-bromobenzylidene)-2,2-dimethyl-1,3-dioxane-4,6-dione (6.22 g, 20 mmol) in DMF (40 mL) under argon atmosphere at 0-5 °C was added by dropwise addition a prepared solution of the dimethylsulfoxonium-methylide from sodium hydride (Alfa Aesar, France) (60% in oil, 880 mg, 22 mmol), trimethylsulfoxonium iodide (Alfa Aesar, France) (4.84 g, 22 mmol) in DMF (60 mL) at room temperature. Upon completion of addition the mixture was stirred at this temperature for a further 30 min. The mixture was then carefully poured onto a stirred mixture of ice/water and ethyl acetate. The crude product was extracted with ethyl acetate, washed well with saturated brine and dried over magnesium sulfate. Filtration and evaporation gave 3.9 g (60% yield) of the crude product as a white solid.

$^1\text{H NMR}$ (300 MHz, CDCl_3) δ 7.51 - 7.44 (m, 2H), 7.23 - 7.17 (m, 2H), 3.39 (t, $J = 9.4$ Hz, 1H), 2.63 (dd, $J = 9.3, 4.9$ Hz, 1H), 2.55 (dd, $J = 9.5, 4.9$ Hz, 1H), 1.72 (d, $J = 9.9$ Hz, 6H).

2-(4-Bromophenyl)-1-(methoxycarbonyl)cyclopropanecarboxylic acid

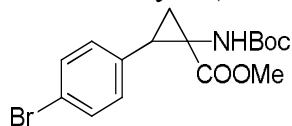


To a suspension of 1-(4-bromophenyl)-6,6-dimethyl-5,7-dioxaspiro[2.5]octane-4,8-dione (3.5 g, 10.77 mmol) in methanol (40 mL) was added a stock solution (85 mL) prepared from potassium hydroxide (Alfa Aesar, France) (1.5 g, 26 mmol) in methanol (200 mL). Upon addition a clear solution ensured and this mixture was stirred for 1 h. the mixture was

evaporated to dryness and the residue taken up into water, filtered and then the filtrate was acidified to pH 3 by the addition of HCl 1N. After extraction and evaporation, 2.88 g (90% yield) of colorless gum was obtained.

$^1\text{H NMR}$ (300 MHz, CDCl_3) δ 7.48 - 7.36 (m, 2H), 7.21 - 7.06 (m, 2H), 3.88 (s, 3H), 3.38 - 3.21 (m, 1H), 2.45 (dd, $J = 8.8, 4.9$ Hz, 1H), 2.21 (dd, $J = 9.5, 4.9$ Hz, 1H).

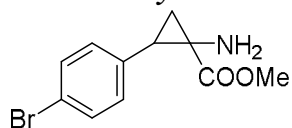
Methyl 2-(4-bromophenyl)-1-((tert-butoxycarbonyl)amino)cyclopropanecarboxylate



To a solution of 2-(4-bromophenyl)-1-(methoxycarbonyl)cyclopropanecarboxylic acid (2.073 g, 6.93 mmol) in *t*-butanol (25 mL) was added diphenylphosphorylazide (Fluorochem, UK) (2.24 mL, 10.40 mmol) and triethylamine (Alfa Aesar, France) (1.93 mL, 13.87 mmol). The mixture was then stirred at 90 °C under argon atmosphere for 48 h. After evaporation of the solvent, the residue was partitioned between ethyl acetate and water. The organic layer was separated and the aqueous layer was extracted with ethyl acetate. The combined organic extracts were washed with brine, dried over magnesium sulfate, filtered and concentrated. The crude product was purified by flash column chromatography using a 90/10 v/v cyclohexane/ethyl acetate as solvent to afford 1.41 g (55% yield) of title compound as a white solid.

$^1\text{H NMR}$ (300 MHz, CDCl_3) δ 7.50 - 7.37 (m, 2H), 7.04 (d, $J = 7.0$ Hz, 2H), 4.58 (bs, 1H), 3.77 (s, 3H), 3.01 - 2.84 (m, 1H), 2.17 - 1.98 (m, 1H), 1.81 - 1.61 (m, 1H), 1.35 (s, 9H).

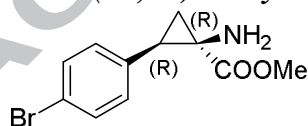
Methyl-1-amino-2-(4-bromophenyl)cyclopropane-1-carboxylate



To a solution of methyl 2-(4-bromophenyl)-1-((tert-butoxycarbonyl)amino)cyclopropanecarboxylate (2.15 g, 5.81 mmol) in DCM (12 mL) was added TFA (Fluorochem, UK) (12 mL) at 0 °C. The mixture was stirred at room temperature for overnight. After evaporation, the residue was dried over high vacuum to give 1.41 g (90% yield) of a white solid.

$^1\text{H NMR}$ (300 MHz, CDCl_3) δ 7.50 - 7.38 (m, 2H), 7.17 - 7.06 (m, 2H), 3.76 (s, 3H), 2.75 (dd, $J = 9.5, 7.6$ Hz, 1H), 1.84 (dd, $J = 9.6, 5.0$ Hz, 1H), 1.60 (bs, 2H), 1.40 (dd, $J = 7.6, 5.0$ Hz, 1H).

(1R,2R) Methyl-1-amino-2-(4-bromophenyl)cyclopropane-1-carboxylate

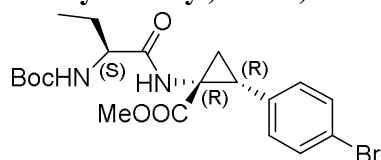


To a solution of methyl-1-amino-2-(4-bromophenyl)cyclopropane-1-carboxylate (9.94 g, 36.81 mmol) in ethyl acetate (65 mL) was added 2,3-dibenzoyl-*L*-tartaric acid (Fluorochem, UK) (13.185 g, 36.81 mmol) followed with 0.34 mL of methanol. The resulting solution was left standing for 2 h until a thick precipitation was formed. The mixture was filtered and the solid was washed with ethyl acetate (6 mL). The solid was stirred in a mixture of 0.1 M sodium carbonate (65 mL) and ethyl acetate (65 mL). The mixture was stirred for 30 min and the two layers were separated. The aqueous layer was extracted two times with ethyl acetate.

The organic layers were combined, dried over magnesium sulfate, and concentrated to afford crude (1*R*,2*R*) methyl-1-amino-2-(4-bromophenyl)cyclopropane-1-carboxylate (4.3 g), which was treated again following the above procedure to give (1*R*,2*R*) methyl-1-amino-2-(4-bromophenyl)cyclopropane-1-carboxylate (3.738 g).

¹H NMR (300 MHz, CDCl₃) δ 7.47 - 7.39 (m, 2H), 7.16 - 7.08 (m, 2H), 3.76 (s, 3H), 2.75 (dd, *J* = 9.5, 7.6 Hz, 1H), 1.83 (dt, *J* = 10.3, 5.2 Hz, 1H), 1.62 (bs, 2H), 1.40 (dd, *J* = 7.6, 5.0 Hz, 1H).

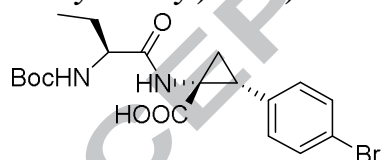
(1*R*,2*R*) Methyl-2-(4-bromophenyl)-1-((*S*)-2-((tert-butoxycarbonyl)amino)butanamido)cyclopropane-1-carboxylate



To a solution of Boc-Abu-OH (Fluorochem, UK) (903 mg, 4.44 mmol) and NMM (0.98 mL, 8.89 mmol) in dichloromethane (36 mL) at 0 °C was added EDCI.HCl (Fluorochem, UK) (1.02 g, 5.33 mmol) and HOBT (817 mg, 5.33 mmol). The reaction mixture was stirred for 1 h at 0 °C, and a solution of (1*R*,2*R*) methyl-1-amino-2-(4-bromophenyl)cyclopropane-1-carboxylate (1.2 g, 4.44 mmol) in dichloromethane (10 mL) was added. The cooling system was removed and the reaction was stirred overnight at room temperature. The solution was poured into a mixture of water and dichloromethane. The organic layer was separated, and the aqueous layer was extracted two times with dichloromethane and two times with ethyl acetate. The organic layers were collected, dried over magnesium sulfate, and concentrated. The residue was purified by flash column chromatography using a 70/30 v/v cyclohexane/ethyl acetate as solvent to afford 1.16 g (57% yield) of title compound as a white solid.

¹H NMR (300 MHz, CDCl₃) δ 7.49 - 7.33 (m, 2H), 7.03 (d, *J* = 8.4 Hz, 2H), 6.13 (bs, 1H), 4.73 (d, *J* = 6.9 Hz, 1H), 3.87 (dd, *J* = 14.0, 6.9 Hz, 1H), 3.73 (s, 3H), 2.95 (t, *J* = 8.9 Hz, 1H), 2.16 (dd, *J* = 9.6, 6.0 Hz, 1H), 1.82 - 1.59 (m, 3H), 1.41 (s, 9H), 0.82 (t, *J* = 7.4 Hz, 3H).

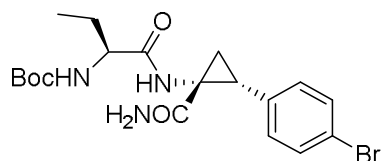
(1*R*,2*R*)-2-(4-Bromophenyl)-1-((*S*)-2-((tert-butoxycarbonyl)amino)butanamido)cyclopropane-1-carboxylic acid



To a solution of (1*R*,2*R*) methyl-2-(4-bromophenyl)-1-((*S*)-2-((tert-butoxycarbonyl)amino)butanamido)-cyclopropane-1-carboxylate (1.37 g, 3 mmol) in THF (10 mL) and water (10 mL) was added LiOH.H₂O (Sigma-Aldrich, France) (378 mg, 9 mmol). The reaction was stirred for 3 h at ambient temperature. After evaporation of THF, the pH value was adjusted to 1 with HCl 1M. The crude product was extracted four times with dichloromethane. The organic layers were collected, dried over magnesium sulfate, and concentrated to afford 1.32 g (quantitative yield) of a white solid.

¹H NMR (300 MHz, CDCl₃) δ 7.43 (d, *J* = 8.4 Hz, 2H), 7.07 (d, *J* = 7.9 Hz, 2H), 6.38 (s, 1H), 4.83 (d, *J* = 7.1 Hz, 1H), 3.87 - 3.80 (m, 1H), 3.02 (t, *J* = 8.9 Hz, 1H), 2.18 (dd, *J* = 9.5, 6.0 Hz, 1H), 1.90 (bs, 1H), 1.80 - 1.64 (m, 2H), 1.43 (s, 9H), 0.80 (t, *J* = 7.3 Hz, 3H).

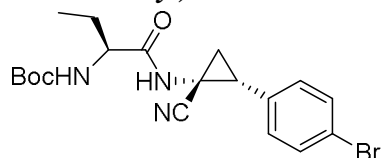
tert-Butyl ((*S*)-1-(((1*R*,2*R*)-2-(4-bromophenyl)-1-carbamoylcyclopropyl)amino)-1-oxobutan-2-yl)carbamate



(1*R*,2*R*)-2-(4-bromophenyl)-1-((*S*)-2-((*tert*-butoxycarbonyl)amino)butanamido)cyclopropane-1-carboxylic acid (1.32 g, 2.98 mmol) was dissolved in dichloromethane (14 mL) and NMM (Sigma-Aldrich, France) (0.66 mL, 5.96 mmol). After the solution was cooled to 0 °C, ethyl chloroformate (Sigma-Aldrich, France) (0.43 mL, 4.47 mmol) was added. The reaction was stirred for 1 h at 0 °C, and the mixture was poured into a flask with 45 mL of ammonia (Sigma-Aldrich, France). The reaction was stirred overnight at ambient temperature. The mixture was extracted three times with dichloromethane and three times with ethyl acetate. The organic layers were collected, dried over magnesium sulfate and concentrated. The crude product was purified by flash column chromatography using a 95/5 v/v dichloromethane/methanol to afford 1.17 g (80 % yield) of a white solid.

¹H NMR (300 MHz, DMSO) δ 8.13 (s, 1H), 7.38 (t, *J* = 7.9 Hz, 2H), 7.26 (s, 1H), 7.18 - 6.95 (m, 4H), 3.54 - 3.39 (m, 1H), 2.81 (t, *J* = 8.4 Hz, 1H), 1.72 - 1.42 (m, 2H), 1.36 (s, 9H), 1.12 - 0.97 (m, 1H), 0.61 - 0.38 (m, 3H).

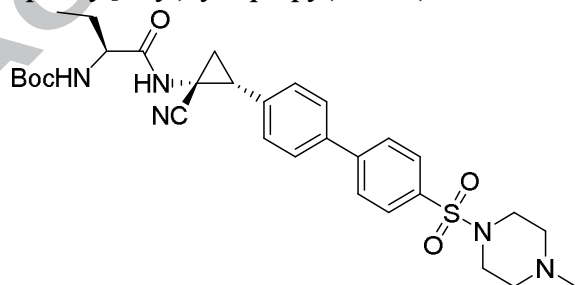
***tert*-Butyl ((*S*)-1-(((1*R*,2*R*)-2-(4-bromophenyl)-1-cyanocyclopropyl)amino)-1-oxobutan-2-yl)carbamate**



To a solution of *tert*-butyl ((*S*)-1-(((1*R*,2*R*)-2-(4-bromophenyl)-1-cyanocyclopropyl)amino)-1-oxobutan-2-yl)carbamate (1.6 g, 3.59 mmol) in DMF (12 mL) was added cyanuric chloride (Sigma-Aldrich, France) (1.65 g, 8.97 mmol). The reaction was stirred for 4 h at ambient temperature. The mixture was partitioned between water and ethyl acetate. The organic layer was collected, washed well with brine, dried over magnesium sulfate, and concentrated. The crude product was purified by flash column chromatography using 65/35 v/v cyclohexane/ethyl acetate to afford 920 mg (57 % yield) of a white solid.

¹H NMR (300 MHz, CDCl₃) δ 7.51 - 7.40 (m, 2H), 7.07 (t, *J* = 8.3 Hz, 2H), 6.49 (bs, 1H), 4.56 (bs, 1H), 3.86 - 3.59 (m, 1H), 2.98 - 2.91 (m, 1H), 2.10 - 2.04 (m, 1H), 1.81 - 1.63 (m, 2H), 1.41 (s, 10H), 0.81 (bs, 3H).

***tert*-Butyl ((*S*)-1-(((1*R*,2*R*)-1-cyano-2-(4'-((4-methylpiperazin-1-yl)sulfonyl)-[1,1'-biphenyl]-4-yl)cyclopropyl)amino)-1-oxobutan-2-yl)carbamate**

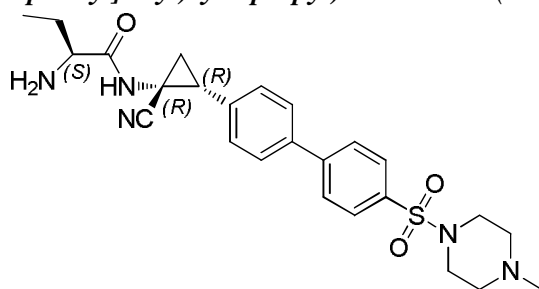


To a solution of *tert*-butyl ((*S*)-1-(((1*R*,2*R*)-2-(4-bromophenyl)-1-cyanocyclopropyl)amino)-1-oxobutan-2-yl)carbamate (1.6 g, 3.74 mmol) in DMSO (48 mL) and H₂O (4.8 mL) was added

1-methyl-4-((4-(4,4,5,5-tetramethyl-1,3,2-dioxaborolan-2-yl)phenyl)sulfonyl)piperazine (1.8 g, 5.61 mmol), potassium carbonate (Sigma-Aldrich, France) (694 mg, 7.48 mmol) and PdCl₂(dppf) (300 mg, 0.47 mmol) under argon atmosphere. The mixture was stirred at 100 °C for 16 h. The mixture was filtered on celite and poured onto ice-water and extracted with ethyl acetate. The organic layer was washed with brine, dried under magnesium sulfate and concentrated. The crude product was purified by flash column chromatography using 95/5 v/v dichloromethane/ methanol to afford 1.52 g (70 % yield) of a white solid.

¹H NMR (300 MHz, CDCl₃) δ 7.81 (d, *J* = 8.3 Hz, 2H), 7.69 (d, *J* = 8.1 Hz, 2H), 7.55 (d, *J* = 8.0 Hz, 2H), 7.30 (d, *J* = 7.5 Hz, 2H), 6.49 (bs, 1H), 4.62 (bs, 1H), 3.76 (t, *J* = 10.8 Hz, 1H), 3.04 (bs, 4H), 2.50 (t, *J* = 4.6 Hz, 4H), 2.28 (s, 3H), 2.13 - 2.11 (m, 1H), 1.82 - 1.77 (m, 1H), 1.42 - 1.24 (m, 11H), 0.77 (bs, 3H).

(*S*)-2-Amino-*N*-((1*R*,2*R*)-1-cyano-2-(4'-((4-methylpiperazin-1-yl)sulfonyl)-[1,1'-biphenyl]-4-yl)cyclopropyl)butanamide (IcatC)



tert-Butyl ((*S*)-1-(((1*R*,2*R*)-1-cyano-2-(4'-((4-methylpiperazin-1-yl)sulfonyl)-[1,1'-biphenyl]-4-yl)cyclopropyl)amino)-1-oxobutan-2-yl)carbamate (1.6 g, 2.75 mmol) was treated with excess of HCOOH (Sigma-Aldrich, France) (20 mL) for 4 h at ambient temperature. The solution was slowly added into a mixture of aqueous NaHCO₃ solution and ice with stirring. After neutralization, the mixture was extracted with ethyl acetate (3 times) and dichloromethane (3 times). The organic layers were collected, dried over magnesium sulfate and concentrated. The crude product was purified by flash column chromatography using 95/5 v/v dichloromethane/ methanol to afford 583 mg (44 % yield) of IcatC as a white solid.

¹H NMR (300 MHz, CDCl₃) δ 7.80 (d, *J* = 8.4 Hz, 2H), 7.68 (d, *J* = 8.4 Hz, 2H), 7.52 (dd, *J* = 11.5, 5.2 Hz, 2H), 7.33 (d, *J* = 8.3 Hz, 2H), 3.18 (dd, *J* = 7.6, 4.8 Hz, 1H), 3.14 - 2.97 (m, 5H), 2.50 (t, *J* = 4.8 Hz, 4H), 2.27 (s, 3H), 2.09 (dd, *J* = 9.7, 7.0 Hz, 1H), 1.91 - 1.78 (m, 1H), 1.67 - 1.09 (m, 4H), 0.65 (t, *J* = 7.5 Hz, 3H).

HRMS (ESI) *m/z*: calcd for C₂₅H₃₂N₅O₃S (M+H)⁺, 482.222037; found, 482.221957

2.2. IC₅₀ determination

The IC₅₀ value of IcatC for human CatC was determined using Gly-Phe-paranitroanilide (Sigma-Aldrich, Denmark) as substrate in 20 mM citric acid, 150 mM NaCl, 2 mM EDTA and pH 4.5. Human CatC (obtained from UNIZYME Laboratories A/S, Denmark) was stored at -20 °C in a buffer containing 2.5 mM Na-phosphate, 150 mM NaCl, 2 mM cysteamine, 50% glycerol, pH 7.0 at a concentration of 1-2 mg/mL (5-10 μM). This stock solution was diluted 500-1000 times in assay buffer to a concentration of 10-20 nM.

The assay was performed in 96-well plates. CatC was added to the well, followed by the test compound in varying concentrations, and the solution was mixed. The plate was incubated at 37°C for 5 minutes, followed by addition of the substrate (750 μ M in the assay) prewarmed to 37°C. The absorption was measured at 405 nm at 37°C for every 90 sec for 12 minutes or every 20 sec for 4 min. IC₅₀ was determined using a 4-parameter logistic equation in a non-linear curve fitting routine.

2.3. *Immunofluorescence*

7 mL peripheral blood samples from healthy control donors and patients with Papillon-Lefèvre syndrome described in ¹⁵ are collected into EDTA preservative tubes by peripheral venipuncture. Samples were taken giving informed consent. Red blood cells lysis took place with water and white cells pelleted with centrifugation for 5 min at 1000 x g. White blood cells were fixed with 2% paraformaldehyde and permeabilized with 0.5% Triton-X 100 (Sigma-Aldrich, USA) in PBS. Non-specific binding sites were blocked with 1% BSA. Primary antibody used at room temperature was rabbit anti-HNE (1:500, 1h). Secondary antibodies was conjugated with Alexa Fluor 488 (Invitrogen, USA) and used at 1:200 dilutions. After incubation, unbound antibody was removed by 3 rinses with PBS. Nuclei were counterstained for 1 min in 0.5 μ g/ml 4,6-diamidino-2-phenylindole (DAPI) before mounting with Moviol 4-88 Reagent (Calbiochem, USA) containing DABCO (Sigma-Aldrich, USA).

2.4. *Bone Marrow*

Samples were taken from six healthy human volunteers giving informed consent. The study was approved by the Ethics committee of the Capital region of Denmark (H-1-2011-165).

15 mL bone marrow was aspirated from the posterior superior iliac crest under local anesthesia and collected in 5 mL sterile acid citrate dextrose (ACD). 20 mL of 2% Dextran 500 in saline was added to induce sedimentation of red cells. The leukocyte-rich supernatant was aspirated and cells were pelleted by centrifugation and resuspended in 180 mL PBS. This suspension was divided in 6 equally sized aliquots that were each under-laid with 15 mL Lymphoprep and centrifuged. Contaminating erythrocytes in the pellet were lysed by hypotonic shock and the leukocytes resuspended in 1 mL MACS buffer (Miltenyi Biotec, Denmark). 20 μ L anti-CD49d were added per 10⁸ cells and the cells were incubated for 15 min, washed and resuspended in 80 μ L MACS buffer per 10⁷ cells. Immunomagnetic anti-IgG

beads were added and CD49d positive cells removed by magnetic absorption.

Cells from the interface were incubated under similar conditions but with anti-CD2, anti-CD3, anti-CD5, anti-CD19, anti-CD56, anti-CD61, and anti-Glycophorin A antibodies to remove non-myeloid cells as previously described²⁵. Samples of both preparations were saved for immunocytochemistry. The remaining cells were resuspended at 1.0×10^7 cells/mL in methionine/cysteine free medium (DMEM) with 10% dialyzed fetal calf serum and divided in equally sized aliquots, one serving as control, the other with IcatC (1 μ M final) added and incubated in parallel for 30 min at 37 °C. The cells were then pelleted and resuspended at 1.0×10^7 cells/mL in identical medium to which ³⁵S methionine/cysteine (EasyTag, Perkin Elmer, Denmark) was added to a final concentration of 200 μ Ci/mL Penicillin and Streptomycin was included. The cells were then incubated for 180 min at 37 °C, washed twice in RPMI and resuspended at 3×10^6 cells/mL in IMDM, containing 20% dialyzed fetal calf serum, penicillin, and streptomycin, 100 ng/mL G-CSF (Granulocyte-colony stimulating factor, Nivestim, Denmark), 50 ng/mL SCF (Stem cell factor, Peprotech, Denmark) and divided in two equal aliquots that were incubated with or without IcatC for up to 5 days.

Cells were pelleted by centrifugation and the supernatant aspirated and mixed with equal volume of 2 x RIPA buffer. The cells were resuspended at 2×10^7 cells/mL in RIPA buffer (150 mM NaCl, 1% (v/v) Triton X-100, 0.1% (w/v) SDS, 1% (w/v) sodium deoxycholate, 30 mM HEPES, pH 7.3). Protease inhibitor (complete mini, Roche), 1 tablet/10 mL RIPA buffer and 1 mM phenylmethylsulphonyl fluoride (Sigma-Aldrich, Denmark) were added. The samples were incubated on ice for 2 hours and cleared by centrifugation at 20,000 x g for 30 minutes. The supernatant was aspirated and subjected to immunoprecipitation. Also, the medium from the chase was subjected to immune precipitation after an equal volume of 2x RIPA buffer with proteinase inhibitors had been added. SDS-sample buffer was added and the samples run on 12% polyacrylamide. The gels were stained with Coomassie, destained, incubated with Amplifier (GE Healthcare, Denmark), dried, placed in a Fuji BAS cassette (Fuji Film), and developed using a Fuji BAS2500 PhosphorImager.

2.5. *Non-human primate experiments*

Female cynomolgus monkeys (*Macaca fascicularis*) (approximately 3 years old and weighing 4-5 kg) were obtained from a commercial supplier. All animal experiments and procedures were approved by the local animal experimentation ethics committee (Comité d'éthique Val de Loire, (APAFIS#2982-20151105293399v6)).

IcatC administration and blood collections- Macaques dosed subcutaneously with IcatC (Mf^(IcatC), 4.5 mg/kg; 5 mL/kg; corresponding to 21 mL of the inhibitor (1.9 mM) resuspended in sterile 15% 2-hydroxypropyl- β -cyclodextrin (HP β CD) solution) or vehicle (15% HP β CD) (Mf^(Cont), 5 mL/kg; corresponding to 24 mL of HP β CD solution) twice daily, after sedation with ketamine (0.35 mg/kg, intramuscular; corresponding to 0.3 mL of Imalgène[®] 1000). HP β CD (Sigma-Aldrich, France) dissolved in 50 mM citrate buffer (pH 5.0) to make a 15% HP β CD solution for injection. Blood samples were collected at days 1, 4, 8, 10 and 12 from the femoral veins into lithium-heparine tubes.

LPS administration- Lipopolysaccharide (LPS) was isolated from *Pseudomonas aeruginosa* serotype 10 (Sigma-Aldrich, France) suspended in sterile water. Monkeys were fasted overnight before sedation with ketamine (0.35 mg/kg, intramuscular; corresponding to <0.3 mL of Imalgène[®]1000). They were anesthetized by isoflurane inhalation (5% vaporizer output). Each monkey was given 100% O₂ for 10 min, its throat was sprayed with 5% xylocaine, and it was intubated with a pediatric endotracheal tube. LPS (0.4 mg/kg) was aerosolized with a microsprinter[®]IA1B (Aerosolizer_IA1B, PennCentury, Philadelphia, PA) connected to a luer-lock 10-mL plastic syringe.

Broncho-alveolar lavage- BAL was performed as a baseline at one day prior to IcatC administration as well as 24 h post-LPS exposure. Monkeys were anesthetized with ketamine (0.35 mg/kg, intramuscular; corresponding to <0.3 mL of Imalgène[®]1000) followed by inhaled isoflurane (5% to induce and 2% to maintain). During anesthesia animals were kept warm under a warming air blanket. Upon anesthetic induction animals were intubated and a flexible Olympus bronchoscope was inserted through an inline adapter in the anesthetic breathing circuit. Sterile saline was instilled and aspirated (3 x 10 mL) through the biopsy channel. BALF recovering 80% of the instilled volume was subsequently centrifuged at 500 x g for 5 min at 4 °C. The cell-free supernatants were concentrated ~20-fold by ultrafiltration. The cells from the pellet were counted and analyzed by flow cytometry.

2.6. Western Blotting

Purified blood neutrophils, white blood cells from blood, or BALF were lysed in lysis buffer (50 mM Tris-HCl, 150 mM NaCl, 1% Nonidet P-40 and 5 mM EDTA) and supernatants were collected after centrifugation. The total protein concentration has been determined by a bicinchoninic acid assay (BCA). The proteins were separated on 12% SDS-polyacrylamide gel electrophoresis (SDS-PAGE) under denaturing conditions (10-50 μ g of

protein per lane). They were transferred to a nitrocellulose (Hybond)-ECL membrane at 4 °C. Free sites on the membranes were blocked by incubation with 5% nonfat dried milk in PBS, 0.1% Tween for 90 min at RT. They were washed twice with PBS, Tween 0.1% and incubated overnight with a primary antibody (a rabbit primary anti-PR3 antibody (1:1000, ab133613²⁶, Abcam, France), a goat primary anti-CatG antibody (1:500, sc-6514, Santa Cruz, Germany), a rabbit primary anti-HNE antibody (1:500, ab1373¹⁹, DAKO, Denmark), a goat primary anti-CatS antibody (1/800, AF1183, R&D Systems, France), a mouse anti-NGAL clone 211.1 (1:500, in-house²⁷) a rabbit primary anti-MPO light chain (1:500, sc-33595, Santa Cruz, Germany) followed by a specific secondary antibody (a goat anti-rabbit IgG secondary antibody (1:7000, Santa Cruz, Germany), a rabbit anti-goat IgG secondary antibody (1:10000, Santa Cruz, Germany)). Membranes were washed (3 x 10 min) with PBS, 0.1% Tween and the detection was performed by ECL system.

2.7. Extravidin-peroxidase detection of active PR3

Cell lysates were incubated with active PR3 probe Bt-[PEG]₆₆-PYDA^P(O-C₆H₄-4-Cl)₂²⁸ (150 nM final) for 30 min at 37 °C in PBS. The reaction was stopped by adding 1 volume of 2 x SDS reducing buffer and heating at 90 °C for 5 min. The samples (10-50 µg) were then separated on 12% SDS-PAGE and transferred to a nitrocellulose membrane at 4 °C. Free sites on the membrane were blocked with 3% bovine serum albumin (BSA) in PBS for 90 min at room temperature (RT). Membranes were then given two quick washes with PBS, Tween 0.1% and incubated for 2 h at RT with extravidin horseradish peroxidase (HRP) (diluted 1/4000 in 3% BSA in PBS, Tween 0.1%). The extravidin-HRP-treated membrane was washed (3 x 10 min) with PBS, Tween 1% and then incubated with HRP substrate for 1 min. Reactive bands were identified by chemiluminescence (ECL kit).

3. Results

3.1. Development and synthesis of a new potent and selective Cat inhibitor, IcatC

A series of peptidyl cyclopropyl nitrile compounds of general formula (I) was synthesized as putative CatC inhibitors (**Figure 2A**). One of these compounds IcatC ((*S*)-2-amino-*N*-((*IR,RS*)-1-cyano-2-(4'-(4-methylpiperazin-1-ylsulfonyl)biphenyl-4-yl)cyclopropyl)butanamide)) (**Figure 2A**) was identified both as the most potent and the most selective inhibitor of *hum*CatC (**Table I**) when compared to a selection of proteases including cysteine cathepsins, neutrophil serine proteases, DPPIV and aminopeptidase N (**Table I**).

Gram amounts of IcatC were required for *in vivo* administration into the macaque and were synthesized through a fourteen-step procedure starting with 4-bromobenzaldehyde and Meldrum's acid and including the separation of the two diastereoisomers (*R,R* and *S,S*) which is a key step in this synthesis. The purified (*R,R*) diastereoisomer (IcatC) (**Figure 2B**) has been characterized by nuclear magnetic resonance (NMR) and high resolution mass spectrometry (HRMS) (**Figure 2C**).

3.2. Biosynthesis and stability of HNE in immature human bone marrow myeloid cells pulse-chased in presence of IcatC

Very small amounts of HNE were observed by confocal microscopy in neutrophils from PLS patients with CatC mutations. The results obtained for one PLS patient are shown in **Figure 3**. We hypothesized that blocking CatC activity could similarly reduce HNE levels. The stability of HNE zymogens was investigated in human bone marrow immature cells pulse-chased up to 5 days in the presence of IcatC.

Bone marrow was aspirated from healthy donors. Immature myeloid cells (blasts, promyelocytes and myelocytes) were separated from the segmented and band cells and most metamyelocytes. Incubation of immature cells with IcatC (1 μ M) does not impair their differentiation which is clearly visible after 24 h and reach 70% of bands cells and segmented cells after 96 h (**Figure 4A**). Immature myeloid cells were then pulsed and chased for 6 h and up to 96 h in the presence or absence of IcatC (1 μ M) (**Figures 4B, and 5A**). Partial degradation of the HNE zymogen was already apparent in lysates of IcatC-treated cells after 6 h of chase and was almost complete after 24 h. However, the low level of constitutively secreted zymogen remained unchanged in supernatants of IcatC-treated as compared to controls (**Figure 5B**). The specific granule protein neutrophil gelatinase-associated lipocalin (NGAL), used here as a reliable, easy to detect, control, remained stable in the lysates of IcatC-treated cells (**Figures 4C, and 5B**) and was secreted with equal abundance by IcatC-treated and non-treated cells (**Figure 5B**). Similar results were obtained for myeloperoxidase (MPO) which is generated at the same stage of maturation as HNE and co-localizes with HNE in azurophil granules (*not shown*). We conclude from these results that the degradation of the elastase zymogen is a very early phenomenon that starts during the differentiation of immature myeloid cells.

We then aimed to inhibit CatC *in vivo* by long term systemic administration of IcatC in a non human primate model, and analyzed the elastase-like protease content in leukocytes from blood and BALF.

3.3. Long-term inhibition of CatC in *Macaca fascicularis*

Preliminary experiments carried out in mice showed that a prolonged administration of IcatC (1.2 to 4.8 mg/kg; twice daily) induced a dose-dependent inhibition of elastase-like proteases in white blood cells lysates. Further no clinical signs of toxicity and no effect on body weight were observed. We tentatively transposed this *in vivo* experiment to *Macaca fascicularis* after checking that IcatC inhibited *Mf*CatC as well as *hum*CatC in neutrophil lysates. We prepared gram amounts of IcatC for a 12 day administration into the macaque (4.5 mg/kg; twice daily). The duration of treatment corresponds to the estimated period of time allowing neutrophils to develop from committed stem cells and thus insures that neutrophils in circulation have been exposed to IcatC at the promyelocyte stage and beyond where elastase-like proteases are formed and stored²⁹. The purification method and the purity of macaque blood neutrophils checked by flow cytometry and by microscopy, were implemented before the study was started (**Figure 6A**). Cross reactivity of the substrates, activity-based probes (ABP) and antibodies used for characterization of three *Mf* elastase-like proteases were also tested before the study. The results obtained for *Mf*PR3 are shown in **Figure 6B, C, D**.

Two macaques having very similar white blood cells counts (~6000-8000 cells/ μ L) and neutrophils percentage were selected for the study. Blood samples were collected from macaques 21, 14 and 7 days before administration of IcatC or vehicle to check that proteolytic activities of elastase-like protease in white cell lysates remained stable. Then macaques were dosed subcutaneously with IcatC ($Mf^{(IcatC)}$) or vehicle (2-hydroxypropyl- β -cyclodextrin (HP β CD)) ($Mf^{(Cont)}$) twice a day during 12 days and blood samples were collected at days 1, 4, 8, 10 and 12, with LPS inhalation at day 11 to analyze elastase-like proteases in white blood cell lysates. IcatC did not affect the white blood cells counts (D12, $Mf^{(Cont)}$: 6600 / $Mf^{(IcatC)}$: 8200 cells/ μ L) and the percentage of lymphocytes, monocytes and neutrophils in peripheral blood as shown by flow cytometry analysis (**Figure 7A**) but the activity of *Mf*NE and *Mf*PR3 was completely abolished in cell-lysates after 10 days of IcatC administration (**Figure 7B**). White blood cell lysates were also used to label proteolytically active *Mf*PR3 using a selective biotinylated *hum*PR3 activity-based probe. No active *Mf*PR3 was detected in cell lysates from $Mf^{(IcatC)}$ treated with the inhibitor during 10 and 12 days (**Figure 7C**). Further, we observed by WB a far lower amount of *Mf*NE and *Mf*PR3 zymogens in cell lysates from $Mf^{(IcatC)}$ as compared with control (**Figure 8**). The amount of CatS and MPO, used here as a markers, was similar in cell lysates from $Mf^{(IcatC)}$ and $Mf^{(Cont)}$.

LPS administration to macaques at day 11 induced an important neutrophil increase in BALFs after 24 h (day 12) both in Mf^(IcatC) and Mf^(Cont) compared to BALF baseline values one day prior to IcatC administration (5-7% neutrophils as in ²⁶). Cell counts in the BALF of Mf^(IcatC) and Mf^(Cont) after exposure to LPS were similar (2.0×10^6 cells/mL vs 2.3×10^6 cells/mL) and the percentage of neutrophils also remained similar (**Figure 9A,B**). However, treatment with IcatC resulted in an almost complete elimination of elastase-like activity in BALF cells lysates from Mf^(IcatC) (**Figure 9C**). WB also found only trace amounts of proteases in cell lysates from Mf^(IcatC) as compared with control samples (**Figure 10**).

4. Discussion

CatC is mainly expressed in hematopoietic cells where it participates in the posttranslational activation of granule-associated serine protease zymogens in the bone marrow ^{12, 13, 30}. Activation of granular serine proteases by CatC occurs through the cleavage of the N-terminal dipeptide which allows the newly generated amino-terminal isoleucyl residue to interact with the aspartic acid residue adjacent to the serine of the active site in the interior of the molecule ¹⁴. This interaction results in a reorientation and remodeling of three flexible surface loops within the activation domain which stabilizes the molecule and renders the active-site pocket of the enzyme accessible to substrates.

Neutrophil elastase-like proteases are synthesized in myeloblasts/promyelocytes, the very early stage of neutrophil maturation. The vast majority of them are targeted to and stored in azurophilic granules ³¹. Previous studies reported that the biosynthesis of neutrophil elastase-like protease zymogens remained unchanged for a certain time in immature myeloid cells from a PLS patient with localization in granules ¹⁹ in spite of the total disappearance of zymogens in mature neutrophil ^{11, 13, 19}. These observations indicated that CatC inactivation promoted zymogen elimination during neutrophil maturation ¹⁹. We hypothesized that inhibition of CatC using a synthetic, cell permeable inhibitor could lead to the same result. Would it be the case, this would be of major pharmacological interest for reducing the intracellular level of elastase-like proteases in neutrophil protease-driven inflammatory diseases ^{1, 4}. A variety of synthetic inhibitors have been synthesized that target CatC ^{20, 21}. IcatC, a cyclopropyl nitrile inhibitor, has been developed and identified here as a very sensitive, selective, cell permeable clinical candidate (Patent Pub. No.: WO/2012/130299). Nitriles inhibitors are reversible inhibitors of cysteine proteases. A nitrile CatC inhibitor, AZD7986 ³², is to be tested in a Phase II clinical trial against COPD. Other nitrile inhibitors,

for example against cathepsin K, already reached the late stage of clinical development for osteoporosis or are marketed as antidiabetic DPPIV inhibitor³².

Pulse-chase experiments that we performed on immature myeloid cells isolated from the bone marrow of healthy donors in the presence of IcatC showed that the HNE zymogen was cleaved into low molecular weight fragments during differentiation before disappearing completely. However, the weak, constitutive secretion of the HNE zymogen by bone marrow precursor cells was not altered by IcatC treatment. Since HNE zymogen is secreted in the medium to the same extent in the presence and absence of CatC inhibitor and in PLS patients¹⁹ degradation of HNE zymogen most likely occurs in nascent azurophilic granules and not in the endoplasmic reticulum/Golgi apparatus.

It is remarkable that immature neutrophilic precursors are able to almost completely degrade elastase-like zymogens when the N-terminal dipeptide sequence is not removed. It seems that a change of conformation of zymogens instructs their degradation in precursor cells rather than any lack of proteolytic activity resulting from persistence in the zymogen state³³. The same phenomenon is also observed when serine proteases are bound to serpins. The zymogen-like conformation of serine proteases in the complex with the serpins makes them susceptible to proteolysis^{11, 34-36}. This is in line with the high level of azurocidin also known as heparin binding protein, seen in neutrophil azurophil granules. Azurocidin is a catalytically inactive member of the serine protease family and displays mutations of critical active site residues, Ser instead of His at position 57, and Gly instead of Ser195 (chymotrypsinogen numbering)³⁷. Our results are the first ever, in any system, showing that pharmacological inhibition of CatC can result in the elimination of the zymogens of elastase-like proteases as observed in PLS patients.

We then examined whether IcatC functions similarly *in vivo*, as we had observed *in vitro* using bone marrow cells. The disappearance of elastase-like protease zymogens was not observed in rodent cells after long-term administration of a CatC inhibitor²⁴. Humans and mice clearly differ both in their number of circulating neutrophils (40–70% in human vs 10–25% in mice) and their elastase-like proteases content and properties³⁸⁻⁴⁰. We chose a non human primate *Cynomolgus* monkey model for monitoring how IcatC administration influences the fate of neutrophil elastase-like proteases. The macaque genome shares about 90% sequence identity with the human genome. Further, enzymatic properties and intracellular levels of these proteases are similar between human and macaque^{39, 41}. We found here that twice-a day subcutaneous administration of IcatC to the macaque leads to a complete inhibition of *MfNE* and *MfPR3* after 10 days. We also observed an almost complete

disappearance of elastase-like zymogens in leukocyte lysates. Further, the percentage of neutrophils, monocytes and lymphocytes in the circulation was not modified by IcatC even after a 12 day administration. Long term administration of a CatC inhibitor has been previously performed in rats but no total inhibition of elastase-like activities was observed in bone marrow and blood cell lysates^{22, 29, 32}. Further, no data were available showing effects of CatC inhibition on the neutrophil content in elastase-like proteases. We show here for the first time that it was possible to block almost completely the maturation of elastase-like proteases and the disappearance of their zymogens *in vivo* as observed in PLS patients.

Next, we studied the consequences of the inhibition of elastase-like proteases on the recruitment of neutrophils in the lung of the IcatC-treated macaque following LPS inhalation. Blood neutrophils lacking elastase-like activities were still able to infiltrate and accumulate into the lung airways. This means that the initiation of neutrophil transmigration during the inflammatory response is not elastase-like dependent. This contradicts the results obtained using CatC-knock out mice which do not show an accumulation of neutrophils at inflammatory sites and the phenotype of periodontitis and hyperkeratosis as PLS patients^{12, 42}. We anticipate that neutrophil recruitment to inflammatory sites functions in PLS patients, explaining why they are resistant to bacterial infections, in particular of the lungs, which individuals with neutrophil disorders typically suffer from¹⁹. Further, neutrophils from patients with PLS do not have a general defect in their bacterial killing activities which are highly redundant^{19, 43}. Oxidative mechanisms, hypochloric acid and antimicrobial peptides appear to be much more effective than neutrophil serine proteases for the defense of bacterial infections^{44, 45}.

Inhibition of bone marrow CatC by IcatC as described here reproduces inhibition and degradation of elastase-like proteases observed in PLS. But the transitory pharmacological inhibition of CatC is expected not to induce the dental and skin clinical symptoms observed in PLS patients since those appear several years after birth. CatC targeting inhibitors may also be applicable to COPD or cystic fibrosis patients in general and to PR3-ANCA associated vasculitis patients, as these inhibitors are expected to eliminate major pathogenic factors, elastase-like proteases and the target antigen of ANCA, in these patients.

Acknowledgments

The authors thank Jérôme Montharu (Laboratory Animal Facilities, Université François Rabelais) for his excellent assistance in primate experimentations. The authors thank also Julien Burlaud-Gaillard (Département des Microscopies, Université François Rabelais) and Dr Julio Vasquez (Fred Hutchinson Cancer Research Center, Seattle) for technical assistance to microscopy analysis, Mrs Charlotte Horn (University of Copenhagen) for performing biosynthesis.

Financial support

This work was supported by institutional funding from INSERM and Université François Rabelais de Tours, by grants from the “Association Vaincre la Mucoviscidose (VLM)” (RF20130500913), the “Région Centre-Val de Loire (Project BPCO-Lyse)”, the “National Institute of Health” (NIH R01 HL130472 to MSH), from “Vilhelm Petersen’s Fund” (7221 to NB), from the “Danish Council for Independent Research” (4183-00024 to NB) and the “European Union’s Horizon 2020 research and innovation program” under grant agreement 668036 (RELENT to DEJ). BK acknowledges the Alexandre von Humboldt Foundation for a short term institutional research training grant (2016).

Authorship contributions

Brice Korkmaz supervised the project.

Brice Korkmaz, Niels Borregaard and Marshall Horwitz participated in the research design. Carla Guarino, Yveline Hamon, Cécile Croix, Anne-Sophie Lamort, Sandrine Dallet-Choisy, Sylvain Marchand-Adam, Thomas Baranek, John Pedersen, Conni Lauritzen, Nathalie Heuzé-Vourc’h and Brice Korkmaz conducted the experiments. Conni Lauritzen and John Pedersen designed, optimized and tested a series of peptidyl cyclopropyl nitrile compounds including IcatC. Adam Lesner, Erhan Firatlı contributed materials. Brice Korkmaz, Niels Borregaard, Marie-Claude Viaud-Massuard, Marshall S. Horwitz, Francis Gauthier, Dieter E. Jenne, Mustapha Si-Tahar performed data analyses. Brice Korkmaz, Francis Gauthier and Niels Borregaard wrote the manuscript. All authors contributed to the writing and revision processes of the manuscript.

Disclosure of conflicts of interest

The authors declare no competing financial interests

REFERENCES

1. Korkmaz B, Horwitz MS, Jenne DE and Gauthier F. Neutrophil elastase, proteinase 3, and cathepsin G as therapeutic targets in human diseases. *Pharmacol Rev.* 2010;62(4):726-759.
2. Dubois AV, Gauthier A, Brea D, Varaigne F, Diot P, Gauthier F, et al. Influence of DNA on the activities and inhibition of neutrophil serine proteases in cystic fibrosis sputum. *Am J Respir Cell Mol Biol.* 2012;47(1):80-86.
3. Schreiber A, Pham CT, Hu Y, Schneider W, Luft FC and Kettritz R. Neutrophil serine proteases promote IL-1beta generation and injury in necrotizing crescentic glomerulonephritis. *J Am Soc Nephrol.* 2012;23(3):470-482.
4. Korkmaz B, Lesner A, Letast S, Mahdi YK, Jourdan ML, Dallet-Choisy S, et al. Neutrophil proteinase 3 and dipeptidyl peptidase I (cathepsin C) as pharmacological targets in granulomatosis with polyangiitis (Wegener granulomatosis). *Semin Immunopathol.* 2013;35(4):411-421.
5. Jerke U, Hernandez DP, Beaudette P, Korkmaz B, Dittmar G and Kettritz R. Neutrophil serine proteases exert proteolytic activity on endothelial cells. *Kidney Int.* 2015;88(4):764-775.
6. Kallenberg CG. Pathogenesis of PR3-ANCA associated vasculitis. *J Autoimmun.* 2008;30(1-2):29-36.
7. Kallenberg CG, Heeringa P and Stegeman CA. Mechanisms of Disease: pathogenesis and treatment of ANCA-associated vasculitides. *Nat Clin Pract Rheumatol.* 2006;2(12):661-670.
8. Jenne DE, Tschopp J, Ludemann J, Utecht B and Gross WL. Wegener's autoantigen decoded. *Nature.* 1990;346(6284):520.
9. Brown GR, McGuire MJ and Thiele DL. Dipeptidyl peptidase I is enriched in granules of in vitro- and in vivo-activated cytotoxic T lymphocytes. *J Immunol.* 1993;150(11):4733-4742.
10. McGuire MJ, Lipsky PE and Thiele DL. Generation of active myeloid and lymphoid granule serine proteases requires processing by the granule thiol protease dipeptidyl peptidase I. *J Biol Chem.* 1993;268(4):2458-2467.
11. Perera NC, Wiesmuller KH, Larsen MT, Schacher B, Eickholz P, Borregaard N, et al. NSP4 is stored in azurophil granules and released by activated neutrophils as active endoprotease with restricted specificity. *J Immunol.* 2013;191(5):2700-2707.
12. Adkison AM, Raptis SZ, Kelley DG and Pham CT. Dipeptidyl peptidase I activates neutrophil-derived serine proteases and regulates the development of acute experimental arthritis. *J Clin Invest.* 2002;109(3):363-371.
13. Pham CT, Ivanovich JL, Raptis SZ, Zehnbauser B and Ley TJ. Papillon-Lefevre syndrome: correlating the molecular, cellular, and clinical consequences of cathepsin C/dipeptidyl peptidase I deficiency in humans. *J Immunol.* 2004;173(12):7277-7281.
14. Jenne DE and Kuhl A. Production and applications of recombinant proteinase 3, Wegener's autoantigen: problems and perspectives. *Clin Nephrol.* 2006;66(3):153-159.
15. Hart TC, Hart PS, Bowden DW, Michalec MD, Callison SA, Walker SJ, et al. Mutations of the cathepsin C gene are responsible for Papillon-Lefevre syndrome. *J Med Genet.* 1999;36(12):881-887.
16. Toomes C, James J, Wood AJ, Wu CL, McCormick D, Lench N, et al. Loss-of-function mutations in the cathepsin C gene result in periodontal disease and palmoplantar keratosis. *Nat Genet.* 1999;23(4):421-424.
17. Papillon M and Lefevre P. Two cases of symmetrically familial palmar and plantar hyperkeratosis (Meleda disease) within brother and sister combined with severe dental alterations in both cases. *Bull Soc Fr Dermatol Syphiligr.* 1924;31(82-87) French.
18. Gorlin RJ, Sedano H and Anderson VE. The Syndrome of Palmar-Plantar Hyperkeratosis and Premature Periodontal Destruction of the Teeth. A Clinical and Genetic Analysis of the Papillon-Lefevre Syndrome. *J Pediatr.* 1964;65(895-908).
19. Sorensen OE, Clemmensen SN, Dahl SL, Ostergaard O, Heegaard NH, Glenthøj A, et al. Papillon-Lefevre syndrome patient reveals species-dependent requirements for neutrophil defenses. *J Clin Invest.* 2014;124(10):4539-4548.

20. Guay D, Beaulieu C, Jagadeeswar Reddy T, Zamboni R, Methot N, Rubin J, et al. Design and synthesis of dipeptidyl nitriles as potent, selective, and reversible inhibitors of cathepsin C. *Bioorg Med Chem Lett*. 2009;19(18):5392-5396.
21. Guay D, Beaulieu C and Percival MD. Therapeutic Utility and Medicinal Chemistry of Cathepsin C Inhibitors. *Curr Top Med Chem*. 2010; 10(7):708-716.
22. Gardiner P, Wikell C, Clifton S, Shearer J, Benjamin A and Peters SA. Neutrophil maturation rate determines the effects of dipeptidyl peptidase 1 inhibition on neutrophil serine protease activity. *Br J Pharmacol*. 2016;173(15):2390-2401.
23. Hamon Y, Legowska M, Herve V, Dallet-Choisy S, Marchand-Adam S, Vanderlynden L, et al. Neutrophilic Cathepsin C Is Matured by a Multistep Proteolytic Process and Secreted by Activated Cells during Inflammatory Lung Diseases. *J Biol Chem*. 2016;291(16):8486-8499.
24. Methot N, Rubin J, Guay D, Beaulieu C, Ethier D, Reddy TJ, et al. Inhibition of the activation of multiple serine proteases with a cathepsin C inhibitor requires sustained exposure to prevent pro-enzyme processing. *J Biol Chem*. 2007;282(29):20836-20846.
25. Mora-Jensen H, Jendholm J, Fossum A, Porse B, Borregaard N and Theilgaard-Monch K. Technical advance: immunophenotypical characterization of human neutrophil differentiation. *J Leukoc Biol*. 2011;90(3):629-634.
26. Hamon Y, Legowska M, Herve V, Dallet-Choisy S, Marchand-Adam S, Vanderlynden L, et al. Neutrophilic cathepsin C is matured by a multi-step proteolytic process and secreted by activated cells during inflammatory lung diseases. *J Biol Chem*. 2016.
27. Kjeldsen L, Koch C, Arnljots K and Borregaard N. Characterization of two ELISAs for NGAL, a newly described lipocalin in human neutrophils. *J Immunol Methods*. 1996;198(2):155-164.
28. Guarino C, Legowska M, Epinette C, Kellenberger C, Dallet-Choisy S, Sienczyk M, et al. New selective peptidyl di(chlorophenyl) phosphonate esters for visualizing and blocking neutrophil proteinase 3 in human diseases. *J Biol Chem*. 2014;289(46):31777-31791.
29. Methot N, Guay D, Rubin J, Ethier D, Ortega K, Wong S, et al. In vivo inhibition of serine protease processing requires a high fractional inhibition of cathepsin C. *Mol Pharmacol*. 2008;73(6):1857-1865.
30. Rao NV, Rao GV and Hoidal JR. Human dipeptidyl-peptidase I. Gene characterization, localization, and expression. *J Biol Chem*. 1997;272(15):10260-10265.
31. Cowland JB and Borregaard N. Granulopoiesis and granules of human neutrophils. *Immunol Rev*. 2016;273(1):11-28.
32. Doyle K, Lonn H, Kack H, Van de Poel A, Swallow S, Gardiner P, et al. Discovery of Second Generation Reversible Covalent DPP1 Inhibitors Leading to an Oxazepane Amidoacetonitrile Based Clinical Candidate (AZD7986). *J Med Chem*. 2016;59(20):9457-9472.
33. Lindmark A, Garwicz D, Rasmussen PB, Flodgaard H and Gullberg U. Characterization of the biosynthesis, processing, and sorting of human HBP/CAP37/azurocidin. *J Leukoc Biol*. 1999;66(4):634-643.
34. Dementiev A, Dobo J and Gettins PG. Active site distortion is sufficient for proteinase inhibition by serpins: structure of the covalent complex of alpha1-proteinase inhibitor with porcine pancreatic elastase. *J Biol Chem*. 2006;281(6):3452-3457.
35. Egelund R, Petersen TE and Andreasen PA. A serpin-induced extensive proteolytic susceptibility of urokinase-type plasminogen activator implicates distortion of the proteinase substrate-binding pocket and oxyanion hole in the serpin inhibitory mechanism. *Eur J Biochem*. 2001;268(3):673-685.
36. Stavridi ES, O'Malley K, Lukacs CM, Moore WT, Lambris JD, Christianson DW, et al. Structural change in alpha-chymotrypsin induced by complexation with alpha 1-antichymotrypsin as seen by enhanced sensitivity to proteolysis. *Biochemistry*. 1996;35(33):10608-10615.
37. Watorek W. Azurocidin -- inactive serine proteinase homolog acting as a multifunctional inflammatory mediator. *Acta Biochim Pol*. 2003;50(3):743-752.
38. Kalupov T, Brillard-Bourdet M, Dade S, Serrano H, Wartelle J, Guyot N, et al. Structural characterization of mouse neutrophil serine proteases and identification of their substrate specificities: relevance to mouse models of human inflammatory diseases. *J Biol Chem*. 2009;284(49):34084-34091.

39. Korkmaz B, Jenne DE and Gauthier F. Relevance of the mouse model as a therapeutic approach for neutrophil proteinase 3-associated human diseases. *Int Immunopharmacol.* 2013;17(4):1198-1205.
40. Relle M, Thomaidis T, Galle PR and Schwarting A. Comparative aspects of murine proteinase 3. *Rheumatol Int.* 2011;31(8):1105-1111.
41. Korkmaz B, Kellenberger C, Viaud-Massuard MC and Gauthier F. Selective inhibitors of human neutrophil proteinase 3. *Curr Pharm Des.* 2013;19(6):966-976.
42. Akk AM, Simmons PM, Chan HW, Agapov E, Holtzman MJ, Grayson MH, et al. Dipeptidyl peptidase I-dependent neutrophil recruitment modulates the inflammatory response to Sendai virus infection. *J Immunol.* 2008;180(5):3535-3542.
43. Pham CT and Ley TJ. Dipeptidyl peptidase I is required for the processing and activation of granzymes A and B in vivo. *Proc Natl Acad Sci U S A.* 1999;96(15):8627-8632.
44. Williams R. Killing controversy. *J Exp Med.* 2006;203(11):2404.
45. Perera NC and Jenne DE. Perspectives and potential roles for the newly discovered NSP4 in the immune system. *Expert Rev Clin Immunol.* 2012;8(6):501-503.
46. Korkmaz B, Hajjar E, Kalupov T, Reuter N, Brillard-Bourdet M, Moreau T, et al. Influence of charge distribution at the active site surface on the substrate specificity of human neutrophil protease 3 and elastase. A kinetic and molecular modeling analysis. *J Biol Chem.* 2007;282(3):1989-1997.
47. Epinette C, Croix C, Jaquillard L, Marchand-Adam S, Kellenberger C, Lalmanach G, et al. A selective reversible azapeptide inhibitor of human neutrophil proteinase 3 derived from a high affinity FRET substrate. *Biochem Pharmacol.* 2012;83(6):788-796.
48. Derache C, Epinette C, Roussel A, Gabant G, Cadene M, Korkmaz B, et al. Crystal structure of greglin, a novel non-classical Kazal inhibitor, in complex with subtilisin. *FEBS J.* 2012;279(24):4466-4478.
49. Korkmaz B, Attucci S, Juliano MA, Kalupov T, Jourdan ML, Juliano L, et al. Measuring elastase, proteinase 3 and cathepsin G activities at the surface of human neutrophils with fluorescence resonance energy transfer substrates. *Nat Protoc.* 2008;3(6):991-1000.
50. Attucci S, Korkmaz B, Juliano L, Hazouard E, Girardin C, Brillard-Bourdet M, et al. Measurement of free and membrane-bound cathepsin G in human neutrophils using new sensitive fluorogenic substrates. *Biochem J.* 2002;366(Pt 3):965-970.

Figure legends

Figure 1: Synthetic schema for the synthesis of IcatC

Figure 2: Chemical structure, HPLC profil and HRMS analysis of IcatC. **A)** Chemical structure of IcatC, (*S*)-2-amino-*N*-((1*R*,2*R*)-1-cyano-2-(4'-(4-methylpiperazin-1-ylsulfonyl)biphenyl-4-yl)cyclopropyl)butanamide. Inserts shows the general formula (I). **B)** The purity of IcatC was checked by HPLC on a C18 cartridge and **C)** its mass was checked by HRMS.

Figure 3: Immunofluorescence confocal microscopy of HNE in healthy control and PLS neutrophils. **A)** Shown is indirect immunofluorescence detection by confocal microscopy of HNE (in green) in healthy and PLS neutrophils. DAPI is used for nuclear counterstaining (in blue). **B)** 3D reconstruction of the confocal image sections showing a very low level of HNE in the neutrophil of PLS patient as compared to those of healthy control. These derived from three distinct experiments. Similar results were obtained with neutrophils from other PLS patients.

Figure 4: Biosynthesis of HNE in immature bone marrow neutrophil precursors pulse-chased with or without IcatC. Bone marrow cells depleted in cells of the non neutrophil lineage were separated into immature cells (less mature than band cells) and mature cells by density centrifugation on Lymphoprep as in Sorensen *et al.*,¹⁹. **A)** Giemsa staining of cytopsin of immature cells from a normal individual incubated with IcatC (1 μ M) during 24 h and 96 h. **B)** Biosynthesis of HNE and **C)** NGAL in immature cells from bone marrow after different times of chase as in Sorensen *et al.*,¹⁹. Briefly, immature myeloid cells were pulsed for 3 h with ³⁵S-Methionine/Cysteine and chased for 16, 40, 64 h in the presence or absence of IcatC (1 μ M). The cells and medium were then separated by centrifugation; cell lysates

were immunoprecipitated with non-specific IgG antibodies coupled to Sepharose beads, then with anti-HNE antibodies coupled to Sepharose beads and finally with anti-NGAL antibodies coupled to Sepharose beads.

Figure 5: Biosynthesis and secretion of HNE from immature bone marrow neutrophil precursors pulse-chased with or without IcatC. **A)** Biosynthesis of HNE and **B)** NGAL, in immature cells after different times of chase in the presence or absence of IcatC (1 μ M). Immature cells were pulsed for 1 h with 35 S-Methionine/Cysteine and chased for 6, 18, 24 h in the presence or absence of IcatC (*left*) or pulsed for 3 h with 35 S-Methionine/Cysteine and chased 96 h in the presence or absence of IcatC (1 μ M) (*right*). Cell lysates were treated as in Figure 4. The medium from the chase was immunoprecipitated following the same procedure. Similar results were found in three independent experiments. The constant band of 76 kDa observed in medium from both control cells and cells treated by IcatC was not revealed by anti- HNE antibodies after WB analysis but may serve here as an internal electrophoretic control.

Figure 6: Cross reactivity analysis of the antibody, activity-based probe (ABP) and FRET substrate developed for *humPR3* against *MfPR3*. **A)** Sideward (SS) versus forward (FS) scatter plot and microscopic analysis of Ficoll-purified macaque blood neutrophils. Purified cells were stained by May-Grunwald-Giemsa, magnification x40. **B)** Western-blot analysis of purified human and macaque neutrophil lysates (10 μ g) using anti-PR3 antibody. **C)** Immune detection of PR3 in macaque neutrophil lysates (10 μ g) using active PR3 ABP Bt-[PEG]₆₆-PYDA^P(O-C₆H₄-4-Cl)₂²⁸. **D)** Hydrolysis of the FRET substrate ABZ-VADnVADYQ-EDDnp⁴⁶ by *humPR3* and *MfPR3*. HPLC C18 analysis of substrate

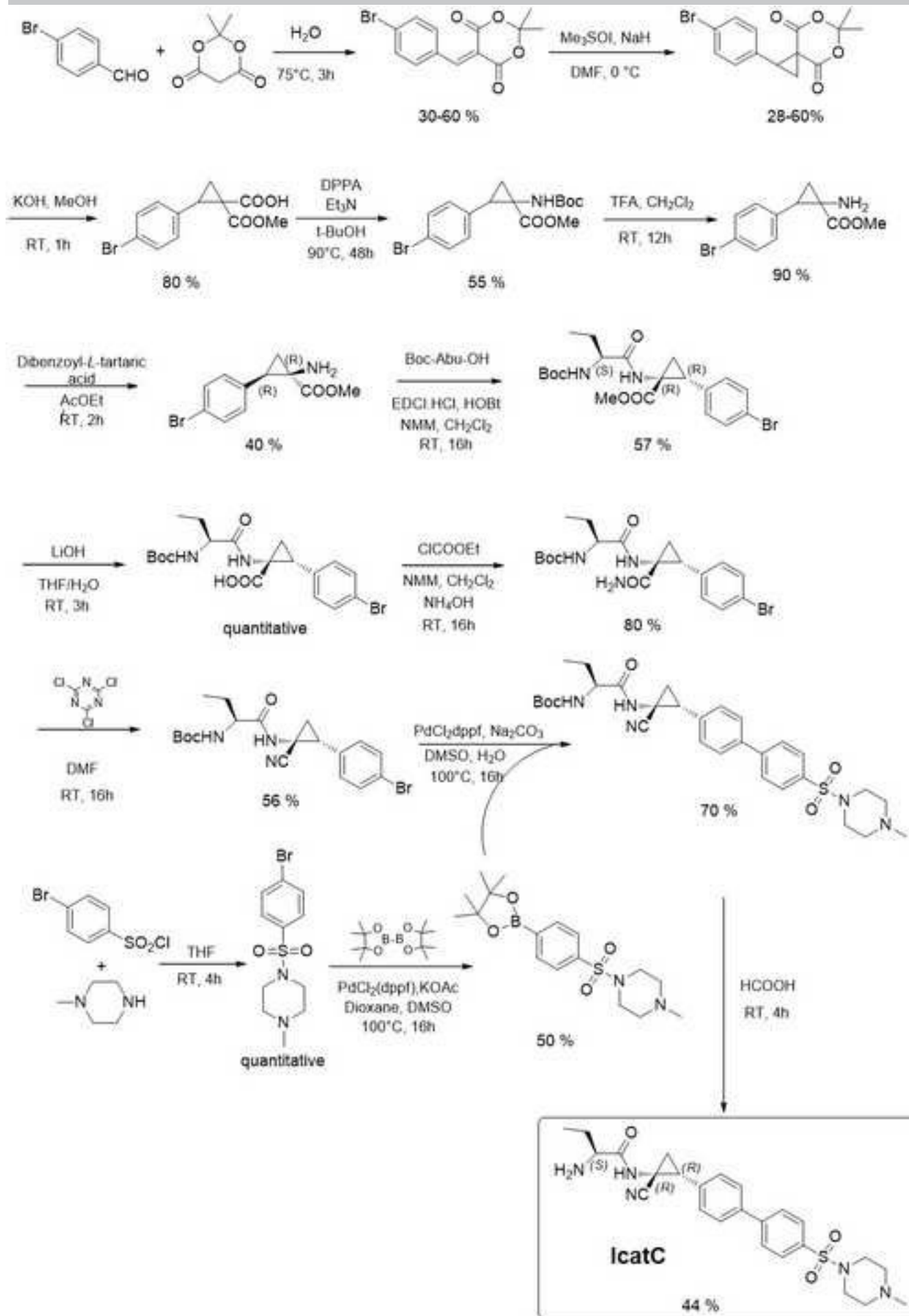
fragments after extensive hydrolysis was performed as in Epinette *et al.*,⁴⁷. Fragments were detected at 220 nm (black), and 360 nm (grey). Similar results were found in three independent experiments.

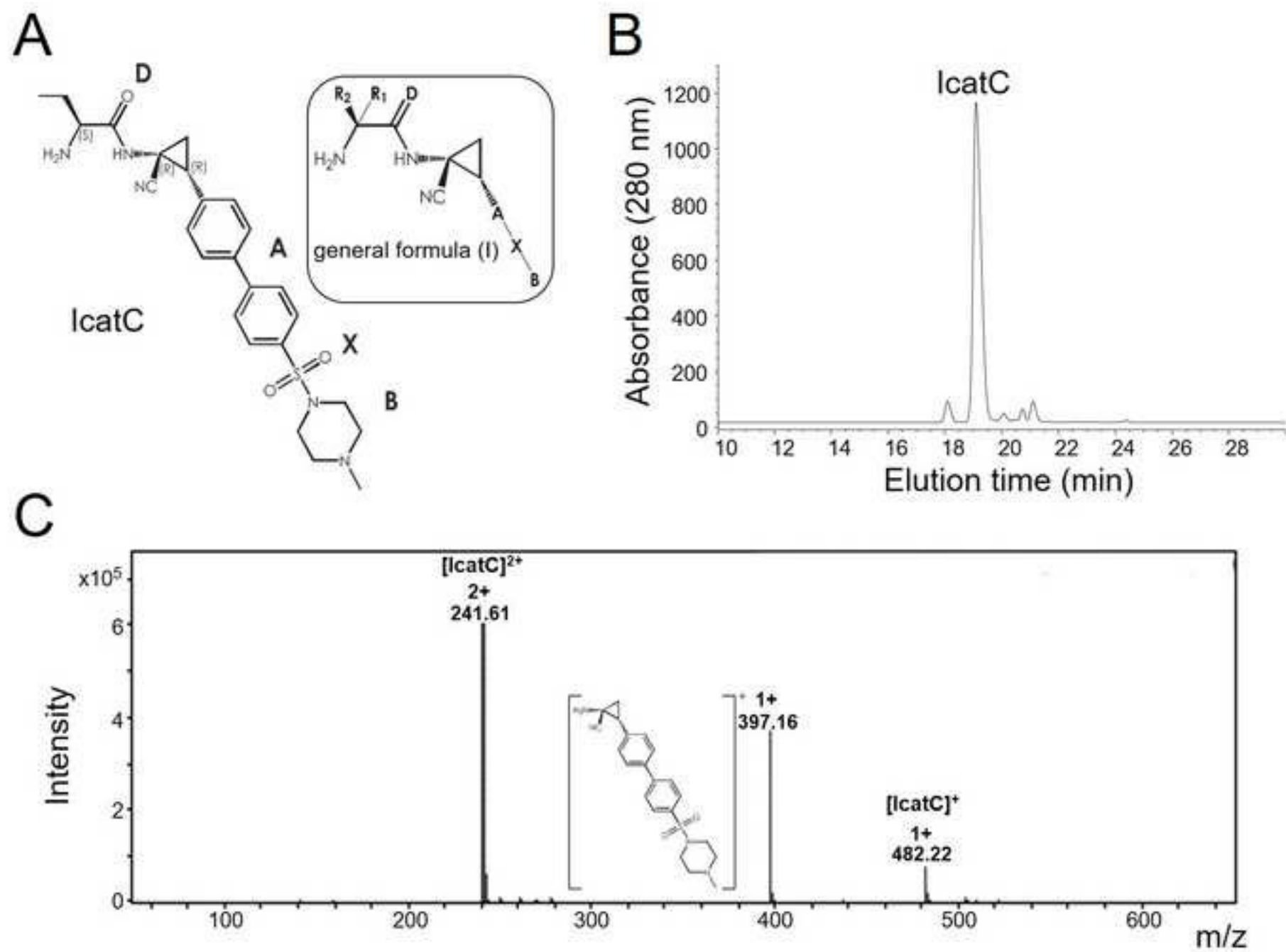
Figure 7: Measurement and immunodetection of elastase-like activities in white blood cells lysates from $Mf^{(Cont)}$ and $Mf^{(IcatC)}$. **A)** Sideward (SS) versus forward (FS) scatter plot of white blood cells from $Mf^{(Cont)}$ (*left*) and $Mf^{(IcatC)}$ (*right*) collected at day 12 (D12). **B)** *Mf*NE, and *Mf*PR3 activities in white blood cells lysates from $Mf^{(Cont)}$ and $Mf^{(IcatC)}$. The cells were lysed in lysis buffer. Soluble fractions were separated from cell debris by centrifugation at 10,000 x g for 10 min. Proteins were assayed with BCA. The proteolytic activities were measured using FRET substrates (elastase substrate: ABZ-APQQIMDDQ-EDDnp⁴⁸ and proteinase 3 substrate: ABZ-VADnorVADYQ-EDDnp⁴⁶ as in Korkmaz *et al.*,⁴⁹) developed for their human homologues using 1 to 10 μ g of white cell lysates from blood samples collected at days 1 (D1), 10 (D10) and 12 (D12) (n=3 measurements, means \pm SD). *FU*, fluorescence unit. Similar results were found in four independent experiments. **C)** Immunodetection of active *Mf*PR3 in white blood cells lysates (50 μ g) using active PR3 ABP Bt-[PEG]₆₆-PYDA^P(O-C₆H₄-4-Cl)₂. Similar results were found in two independent experiments.

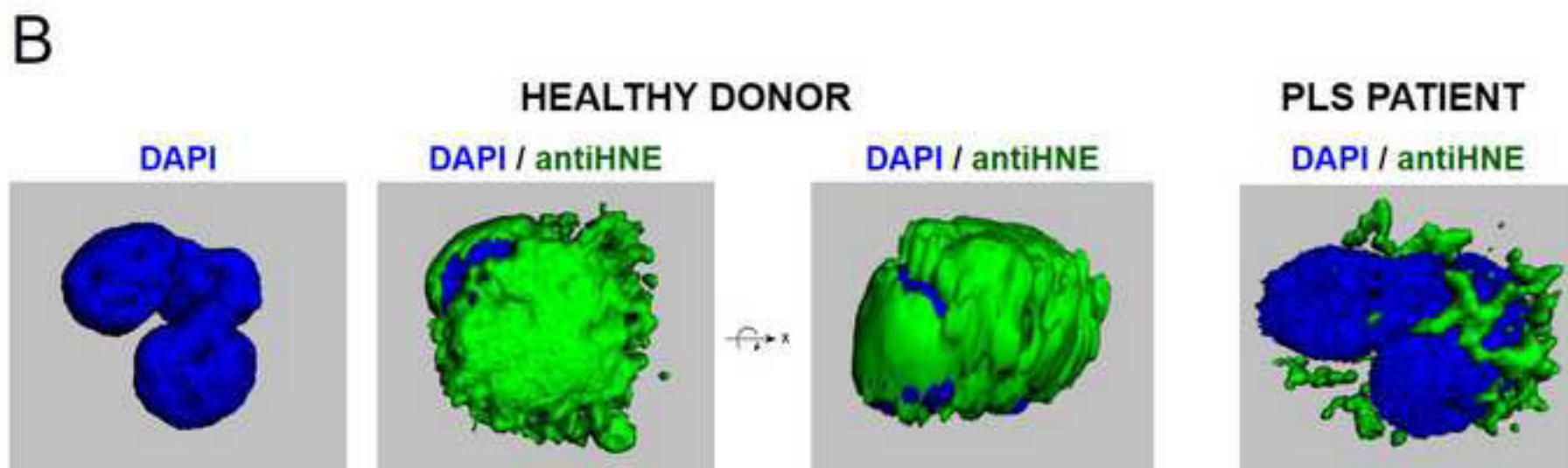
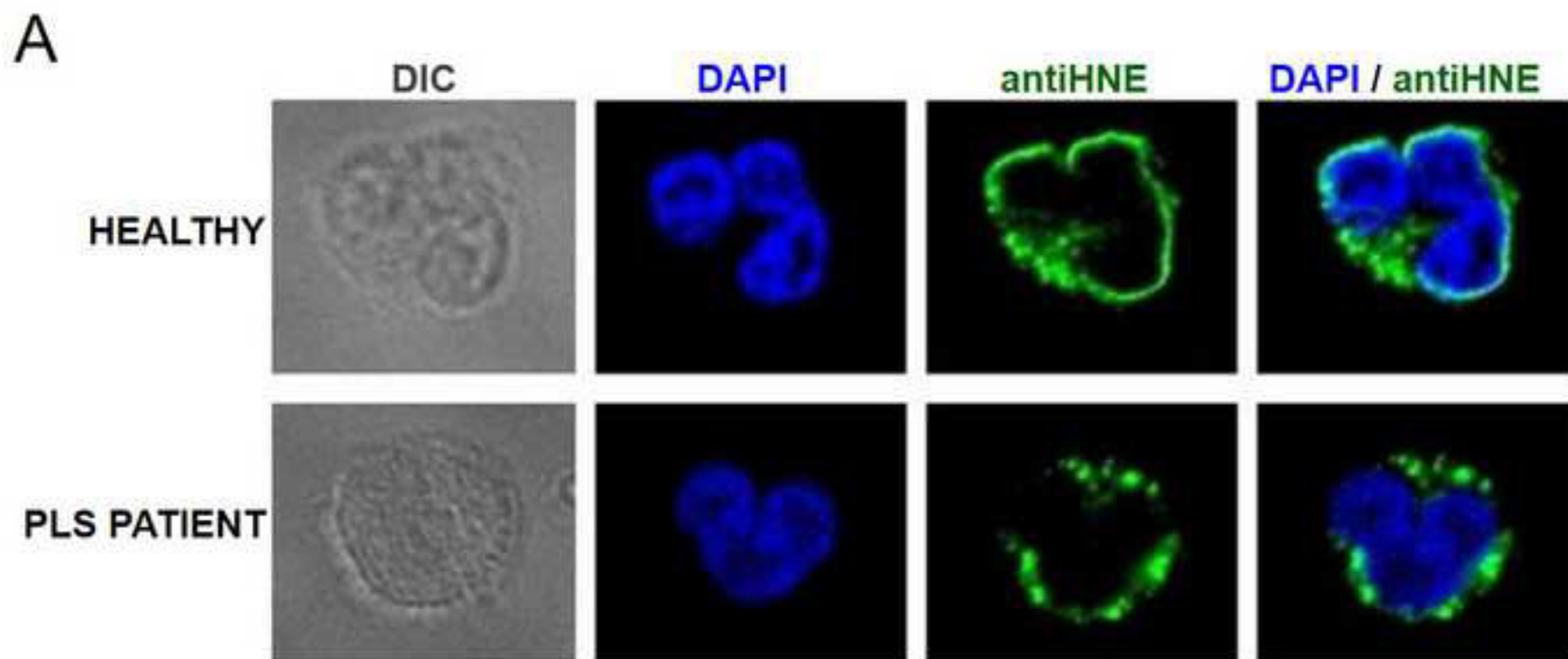
Figure 8: Incidence of CatC inhibition on the protein levels of *Mf*NE and *Mf*PR3 in white blood cells lysates $Mf^{(Cont)}$ and $Mf^{(IcatC)}$. Western-blot analysis of macaque white blood cell lysates (50 μ g) using **A)** anti-NE and **B)** anti-PR3 antibodies showing the almost complete elimination of immunoreactive *Mf*NE and *Mf*PR3 at D10 and D12 post inhibition. Anti-CatS and anti-myeloperoxidase (MPO) used here as control. Similar results were found in three independent experiments.

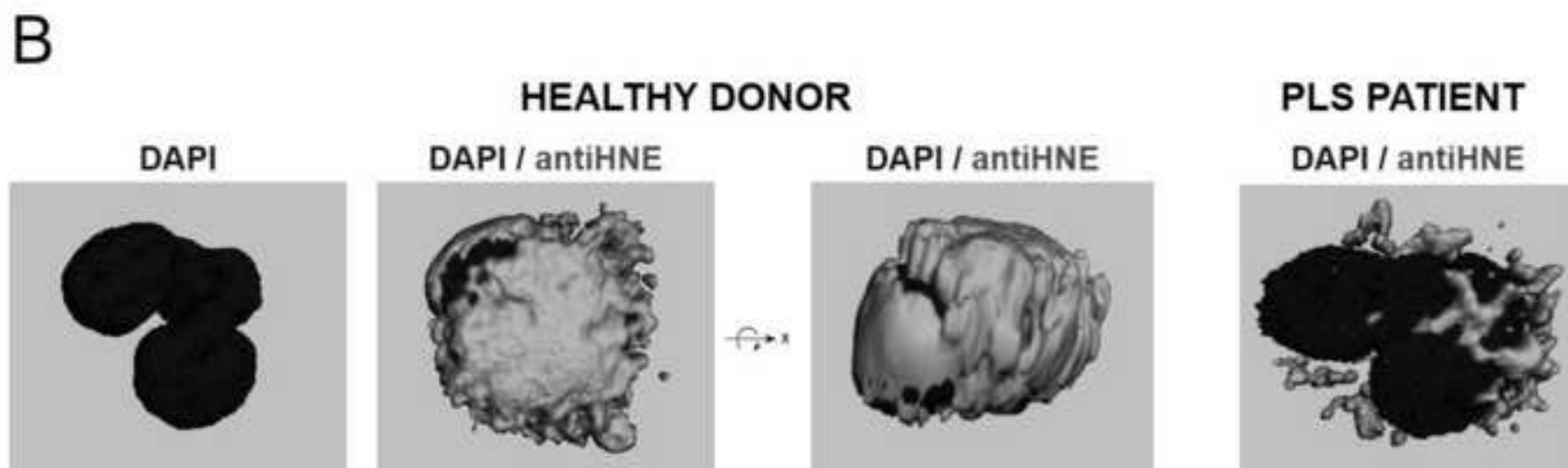
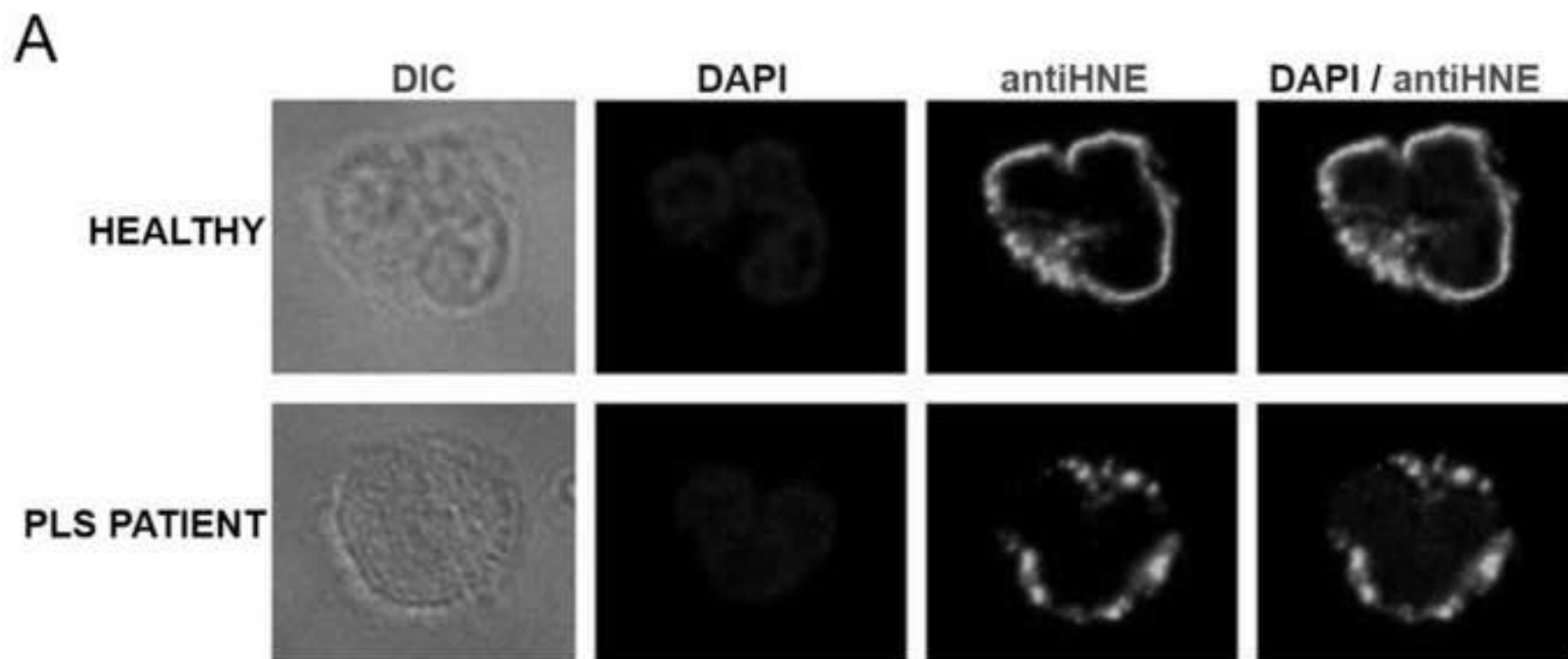
Figure 9: Consequences of the inhibition of elastase-like proteases on the lung neutrophil recruitment in response to induced inflammation. **A)** Sideward (SS) versus forward (FS) scatter plot of BALF cells from $Mf^{(Cont)}$ (left) and $Mf^{(IcatC)}$ (right) collected at day 12. **B)** Microscopic analysis of BALF cells from $Mf^{(Cont)}$ and $Mf^{(IcatC)}$ stained by May-Grunwald-Giemsa, magnification x40. **C)** Measurement and immunodetection of elastase-like activities in BALF cells lysates from $Mf^{(Cont)}$ and $Mf^{(IcatC)}$. Mf/NE , $Mf/PR3$ and $Mf/CatG$ activities in BALF cells lysates from $Mf^{(Cont)}$ and $Mf^{(IcatC)}$ as measured using FRET substrates (ABZ-APQQIMDDQ-EDDnp⁴⁸, ABZ-VADnorVADYQ-EDDnp⁴⁶, ABZ-TPFSGQ-EDDnp⁵⁰ as in Korkmaz *et al.*⁴⁹) developed for their human homologues (n=3 measurements, means \pm SD). *FU*, fluorescence unit. Similar results were found in three independent experiments.

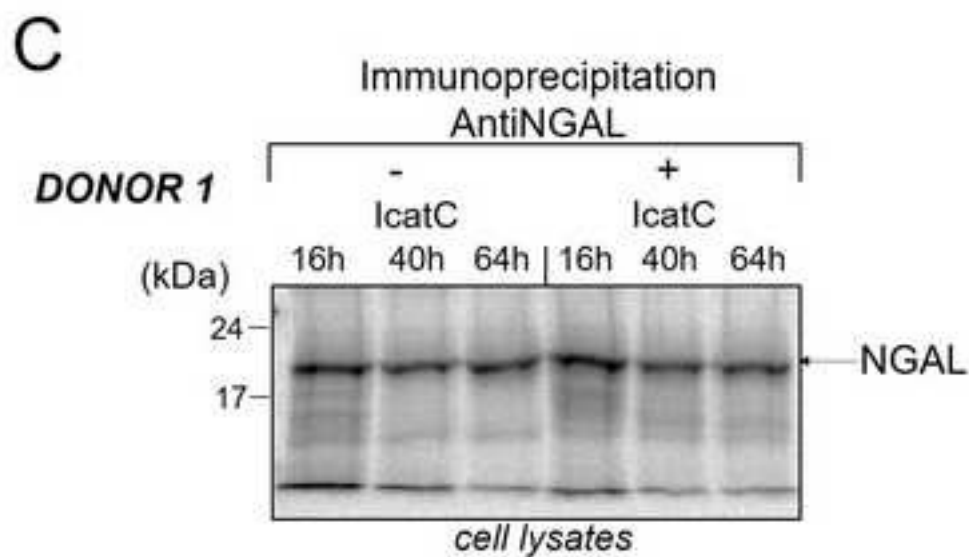
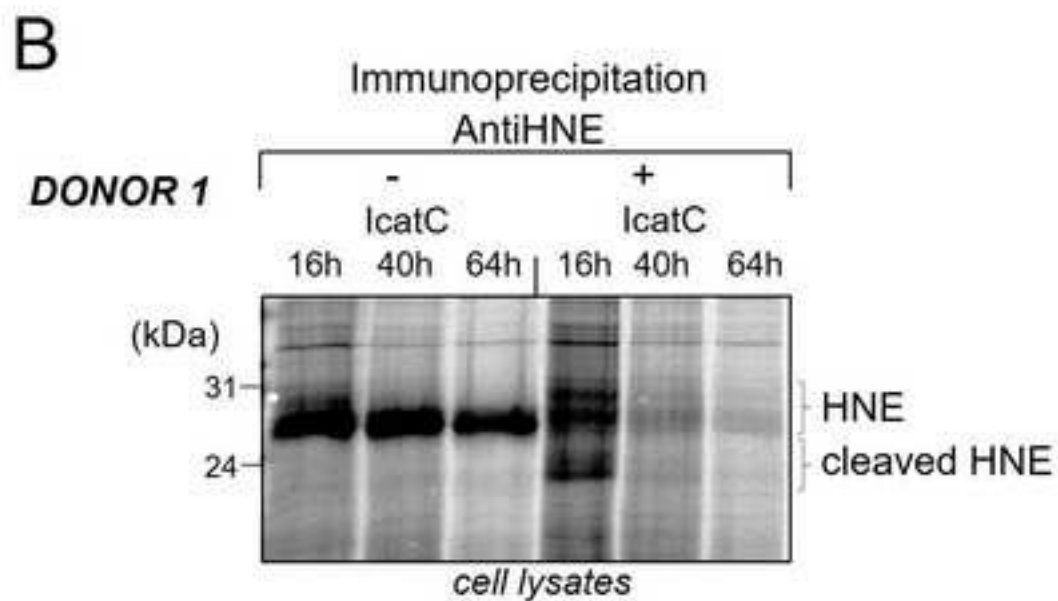
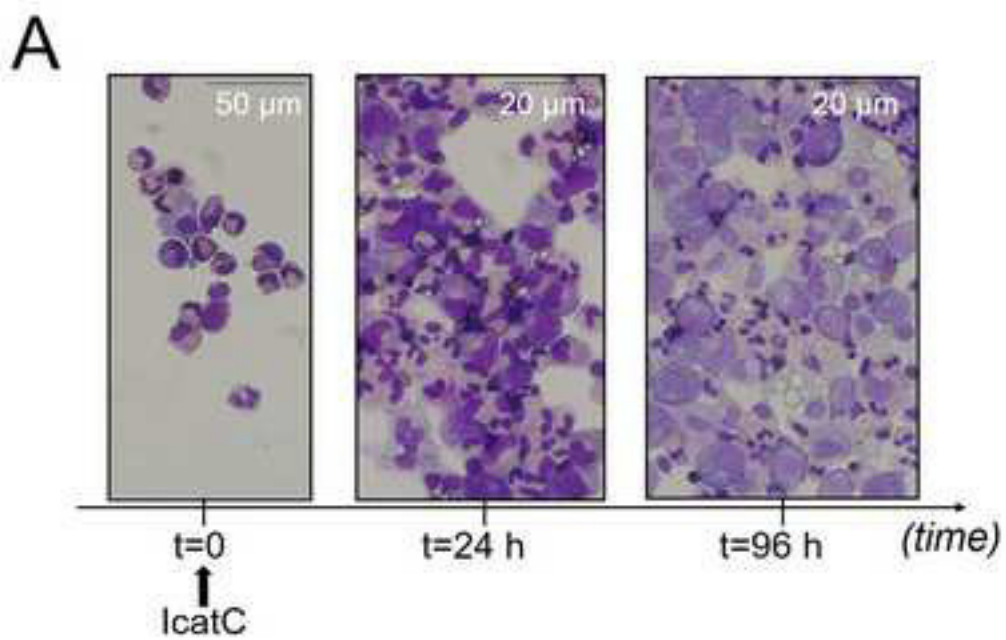
Figure 10: Incidence of CatC inhibition on the protein level and activity of PR3 in BALF cells lysates. **A)** WB analysis of BALF cells lysates from $Mf^{(Cont)}$ and $Mf^{(IcatC)}$ at D12 using anti-PR3 antibodies showing the almost complete elimination of immunoreactive $Mf/PR3$. Anti-myeloperoxidase (MPO) used here as a control of neutrophil content. **B)** Detection of active $Mf/PR3$ in BALF cells lysates (50 μ g) using activity based-probe Bt-[PEG]₆₆-PYDA^P(O-C₆H₄-4-Cl)₂.

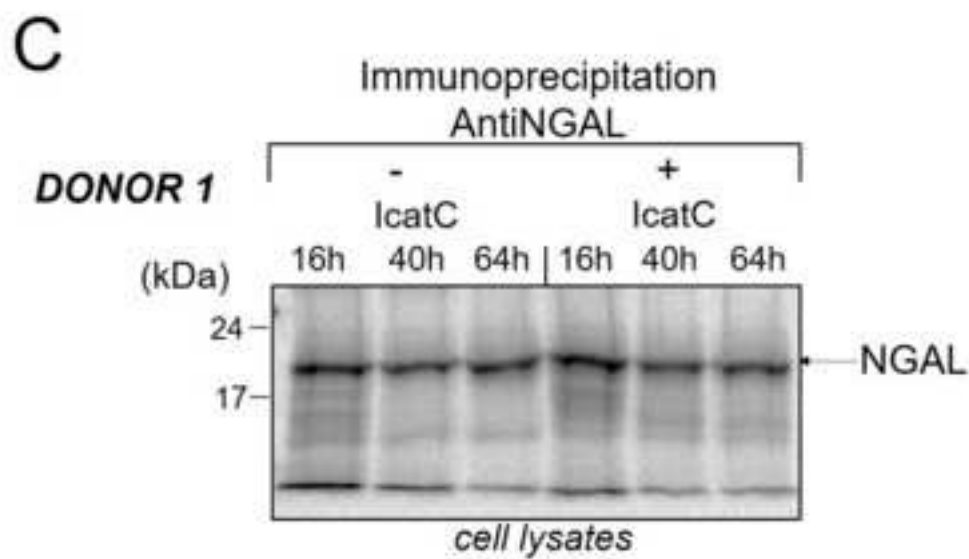
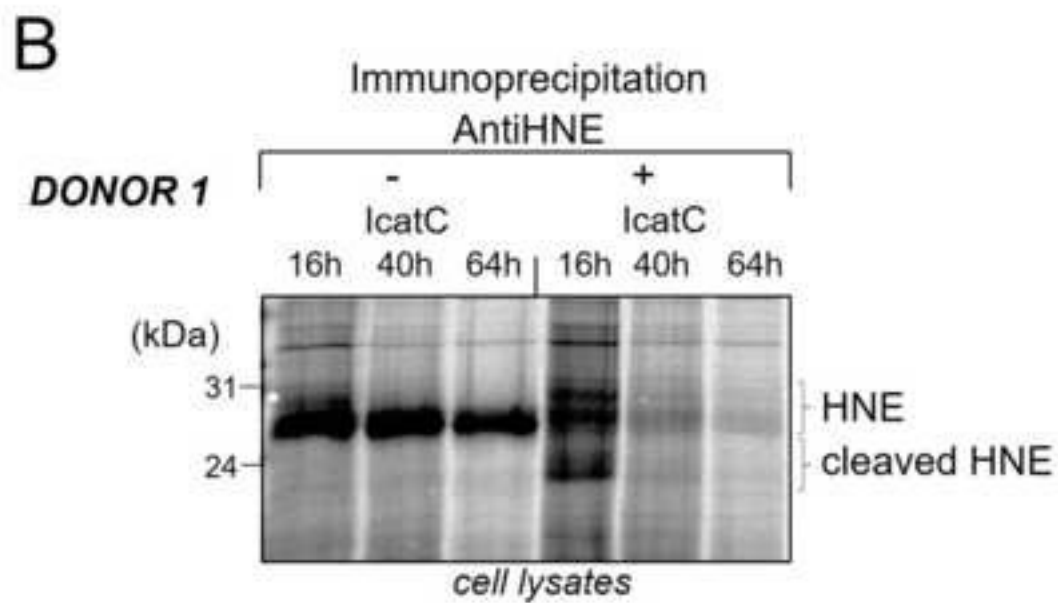
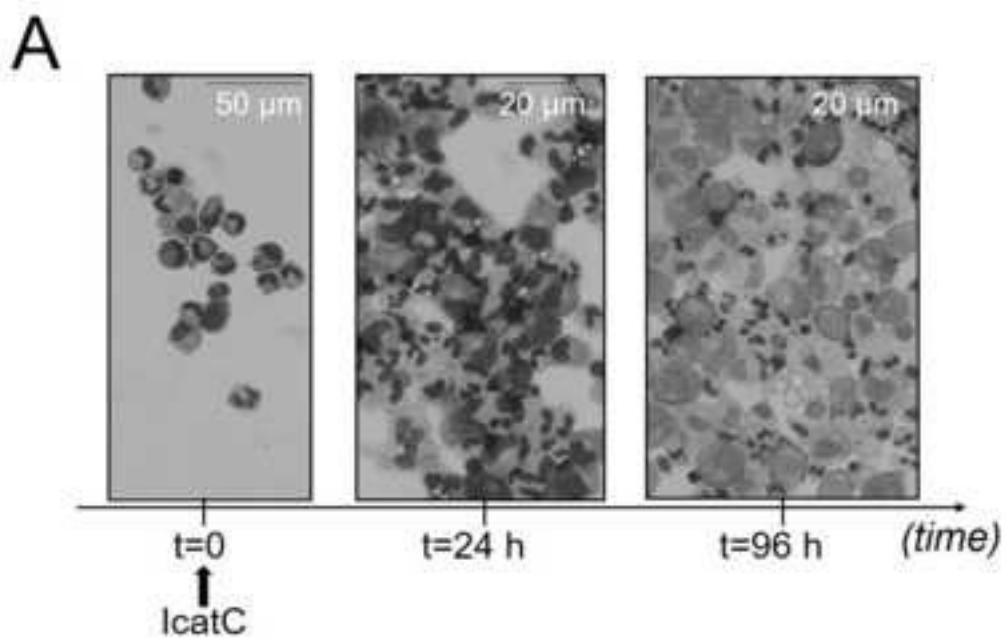


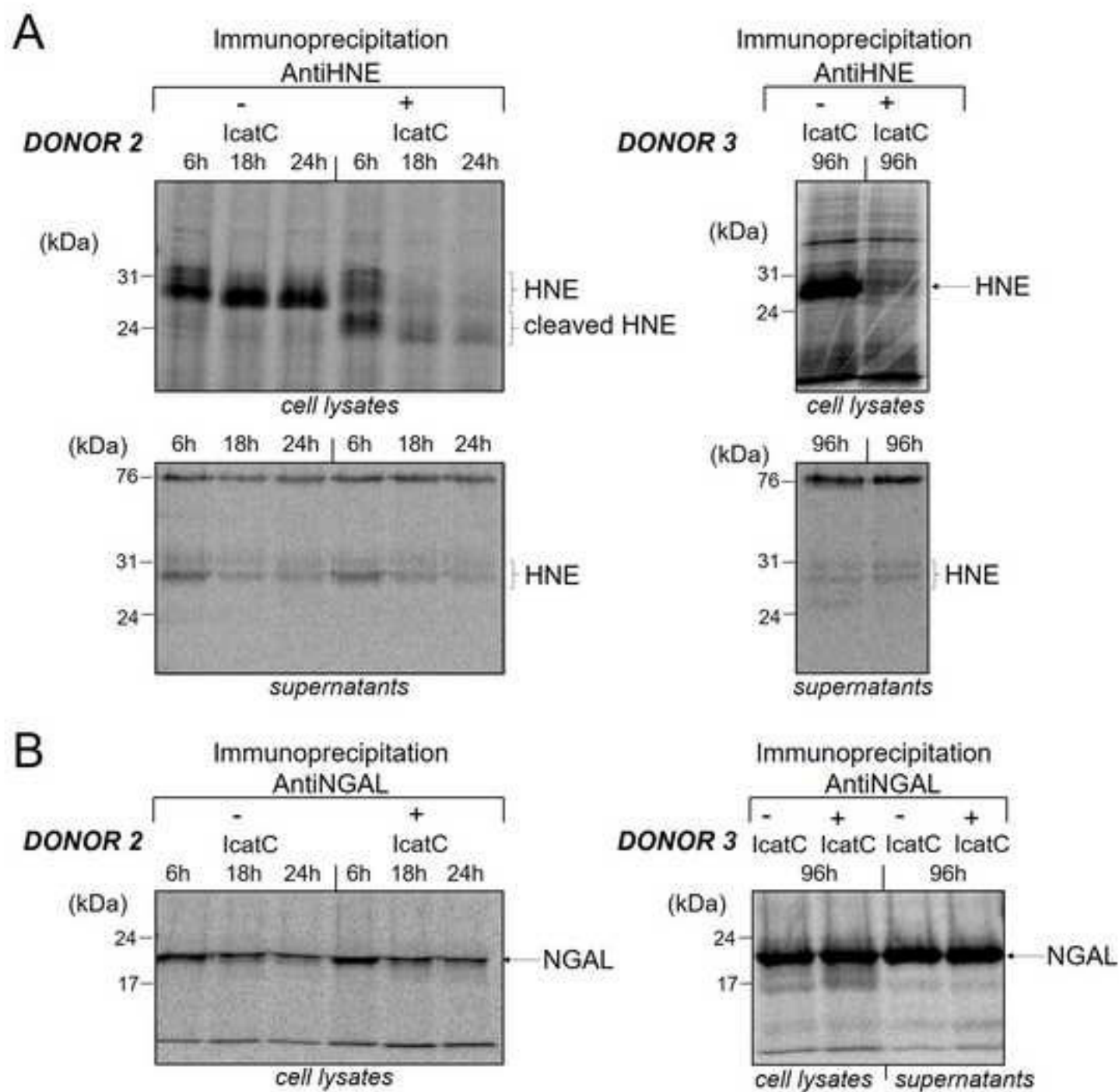


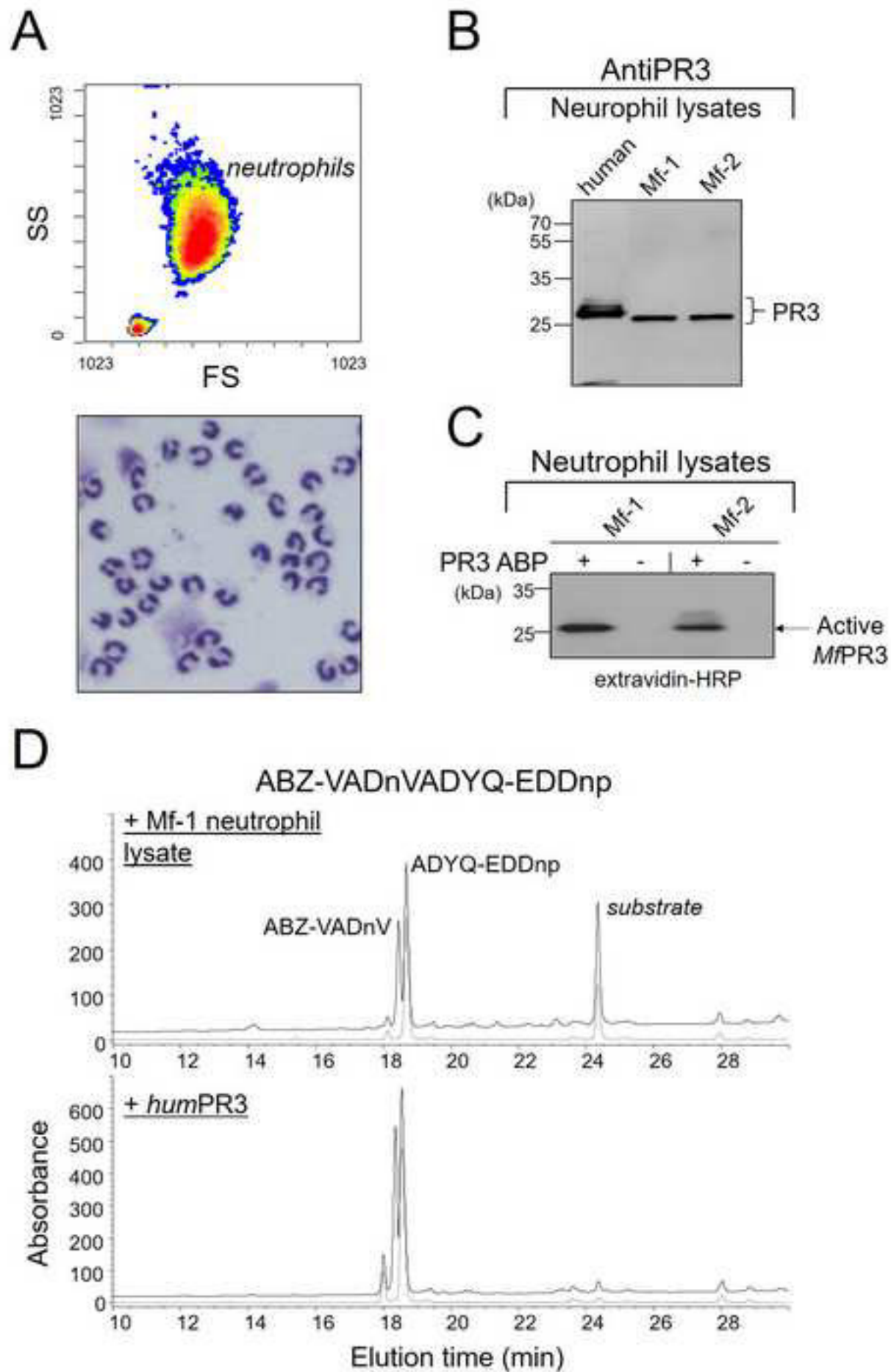


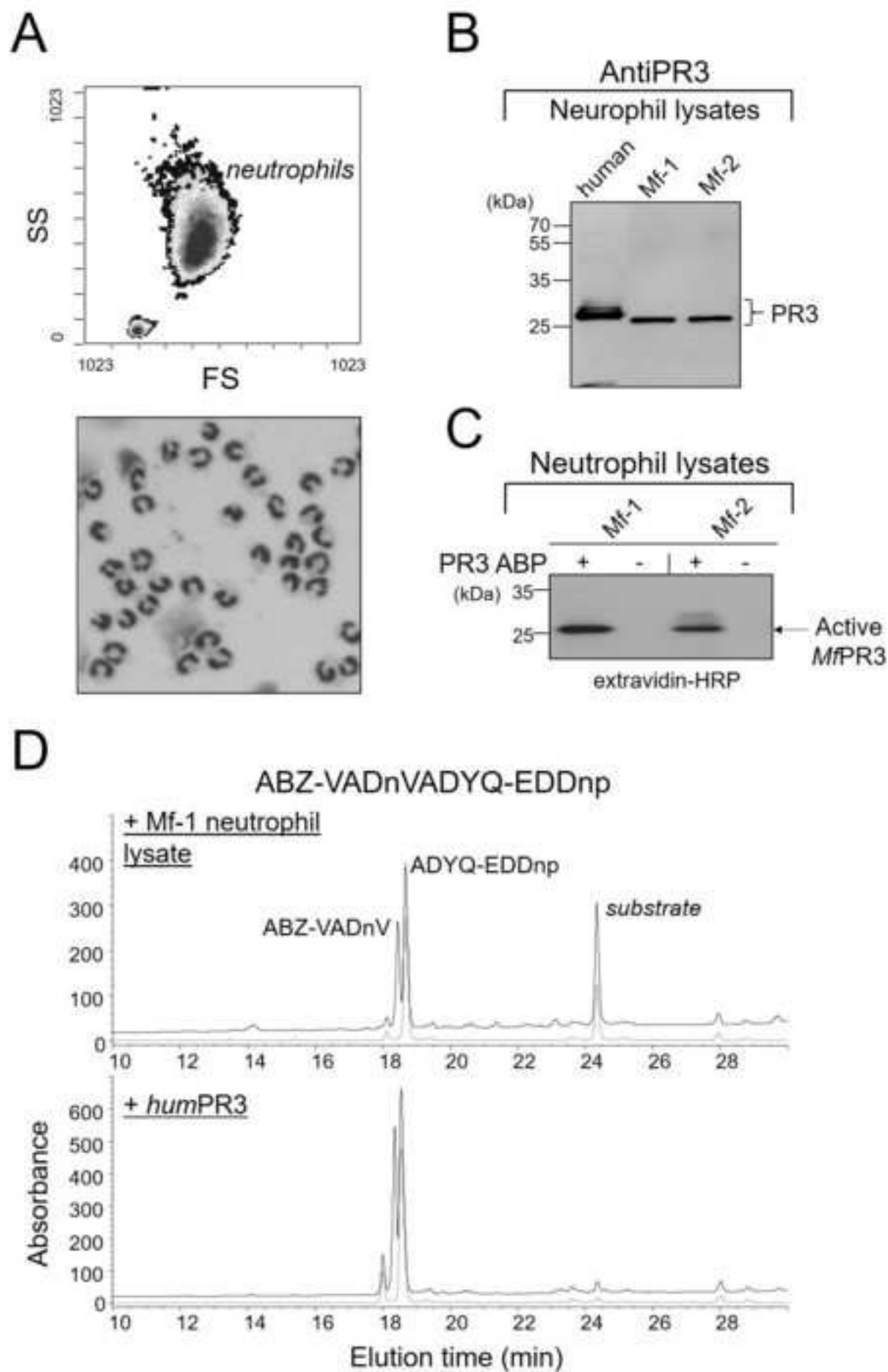


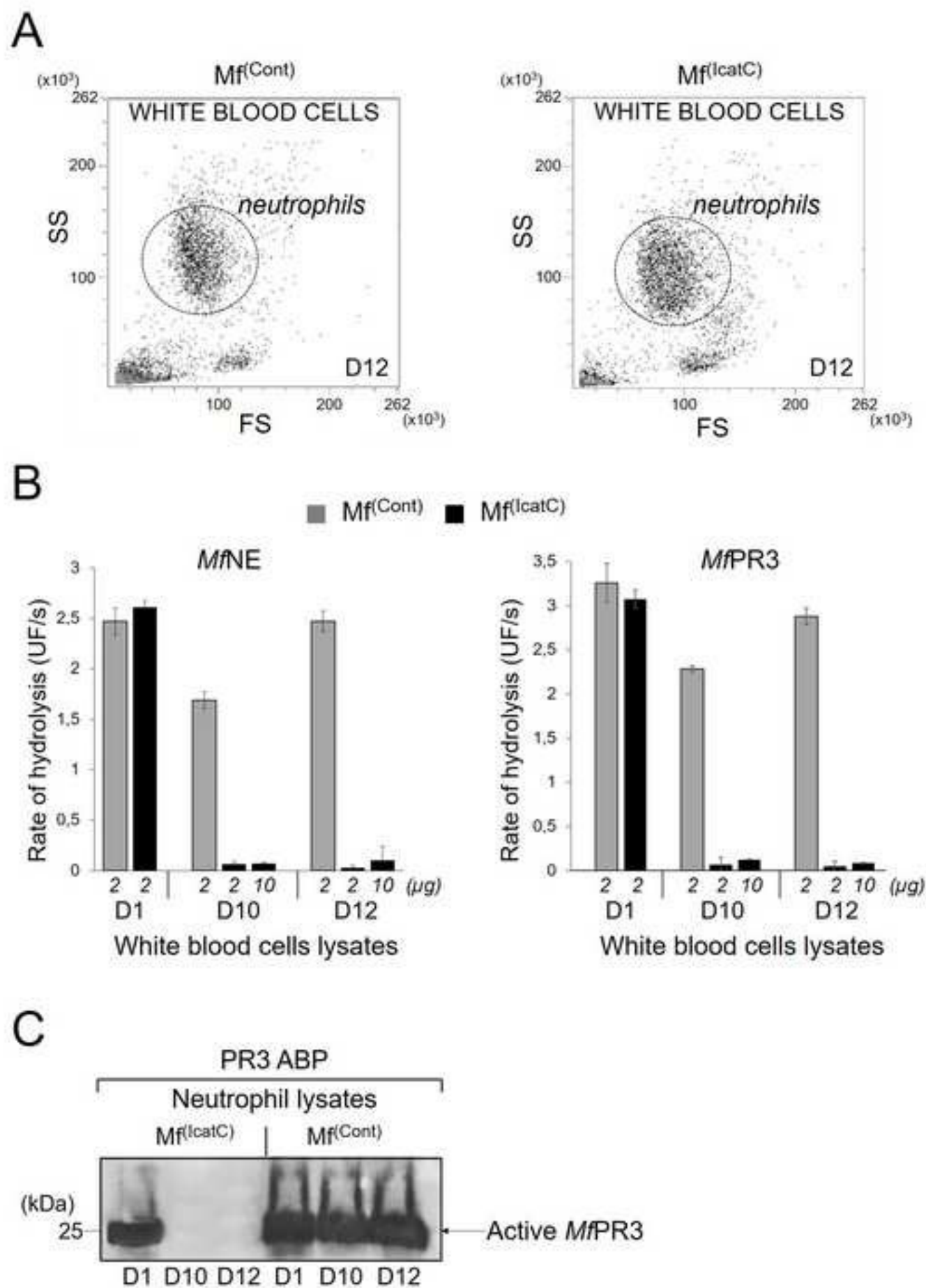


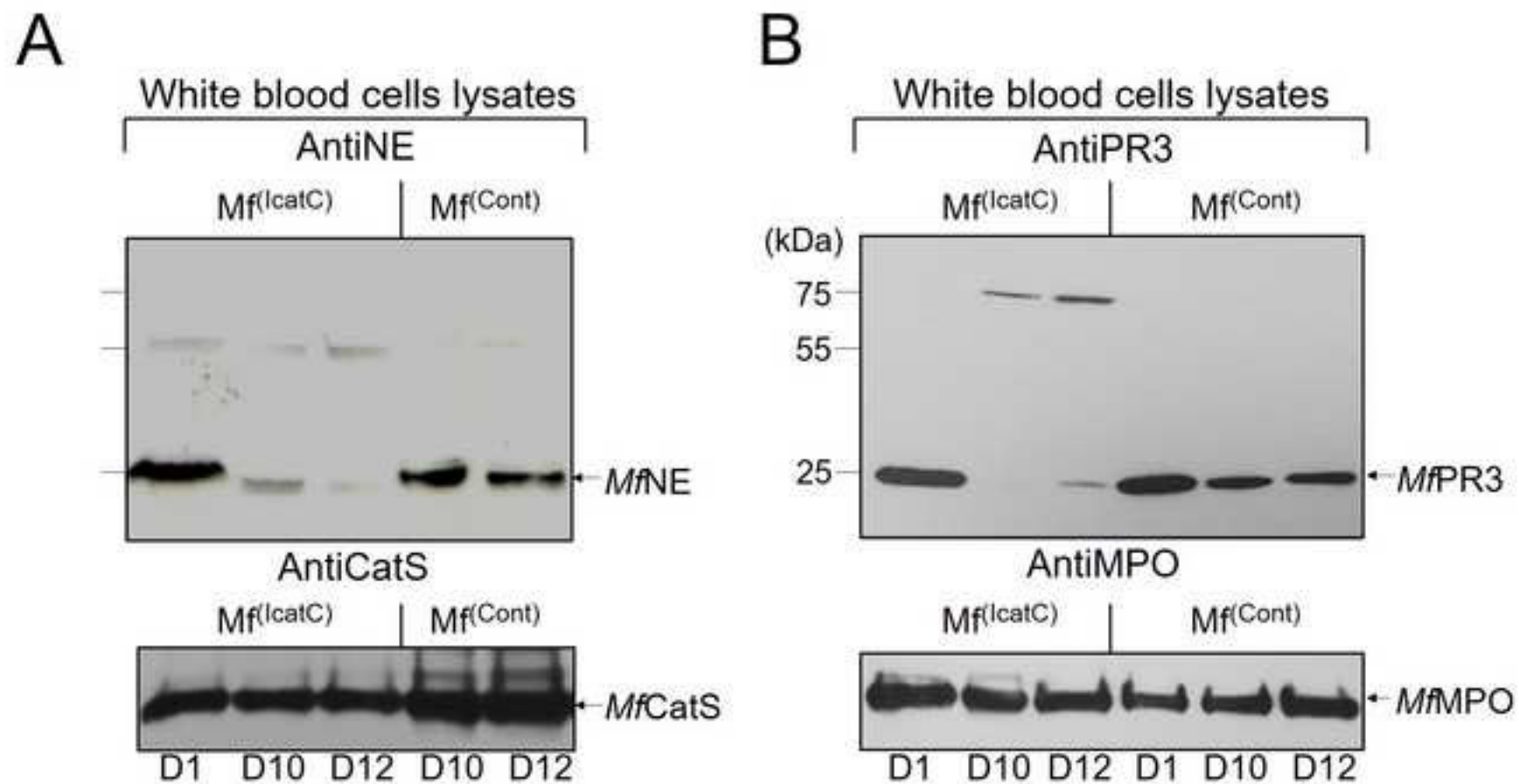


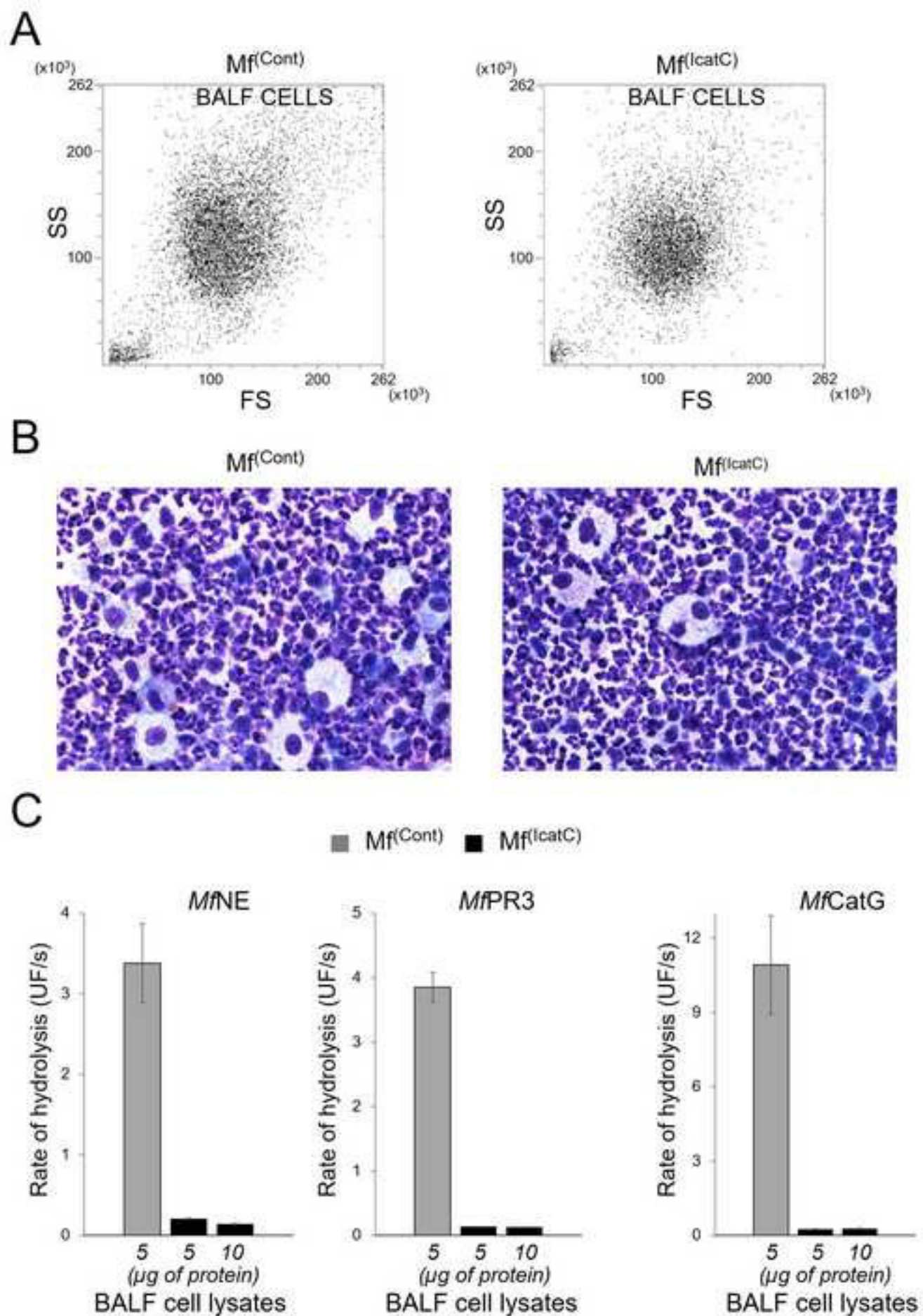


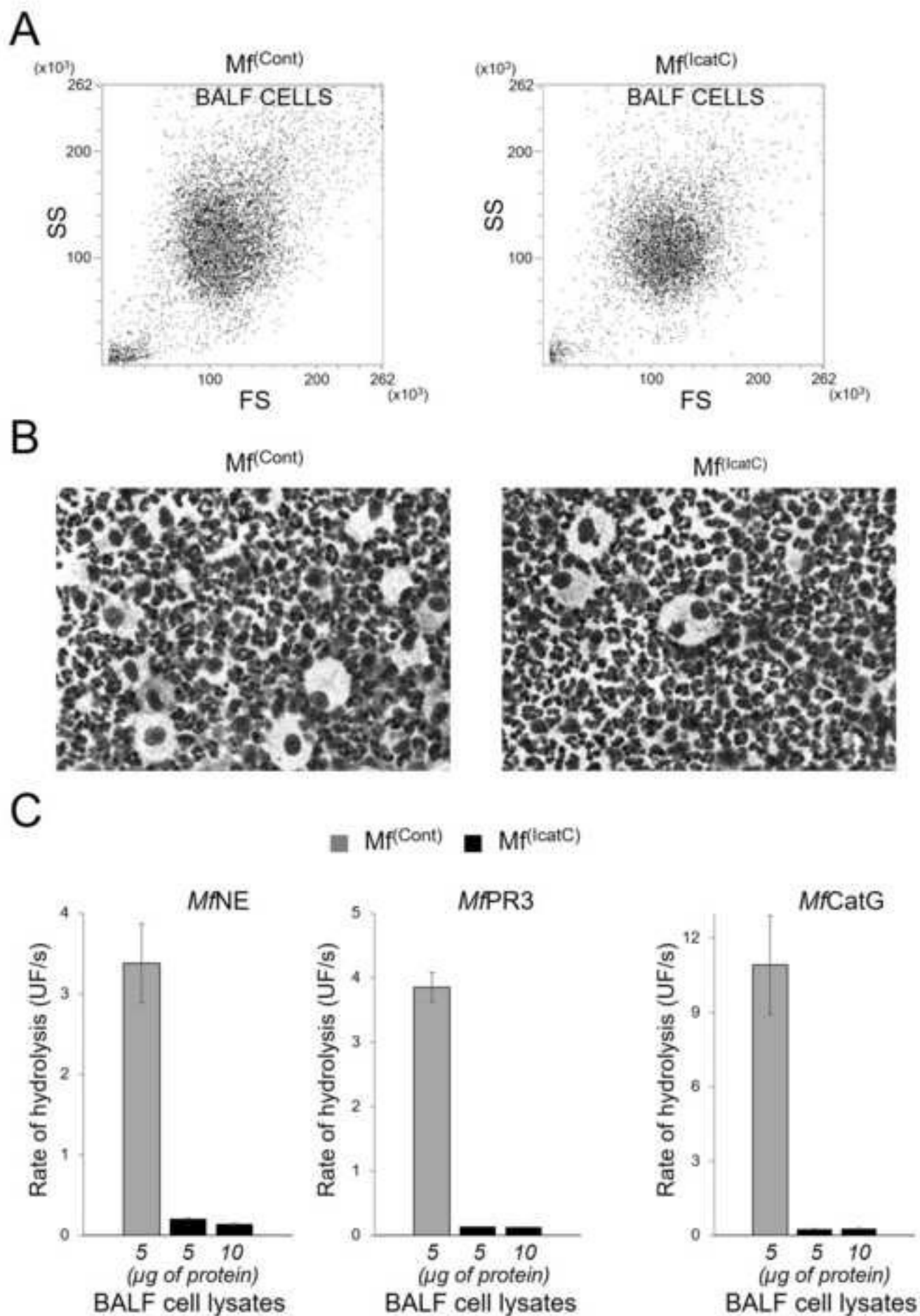


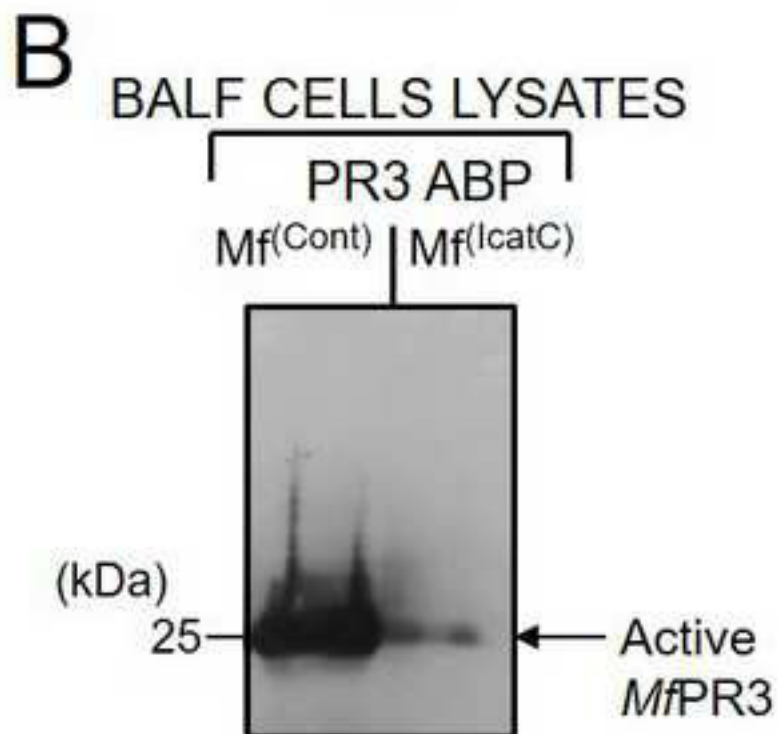
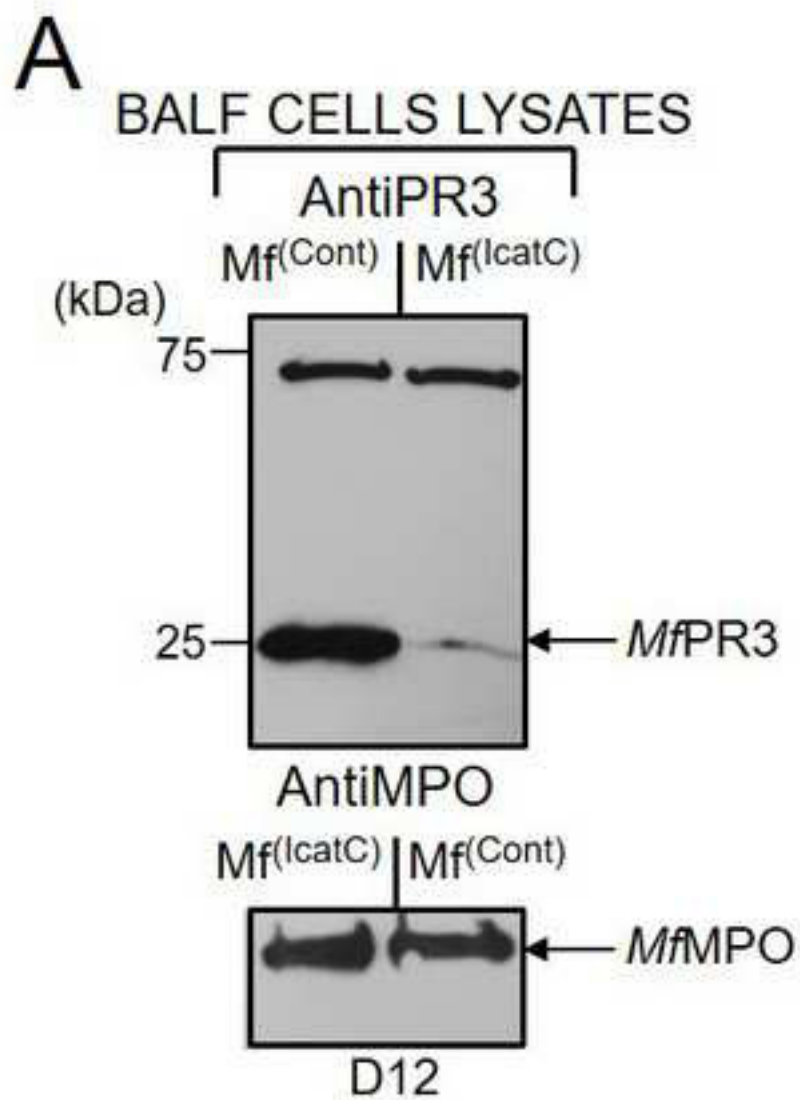


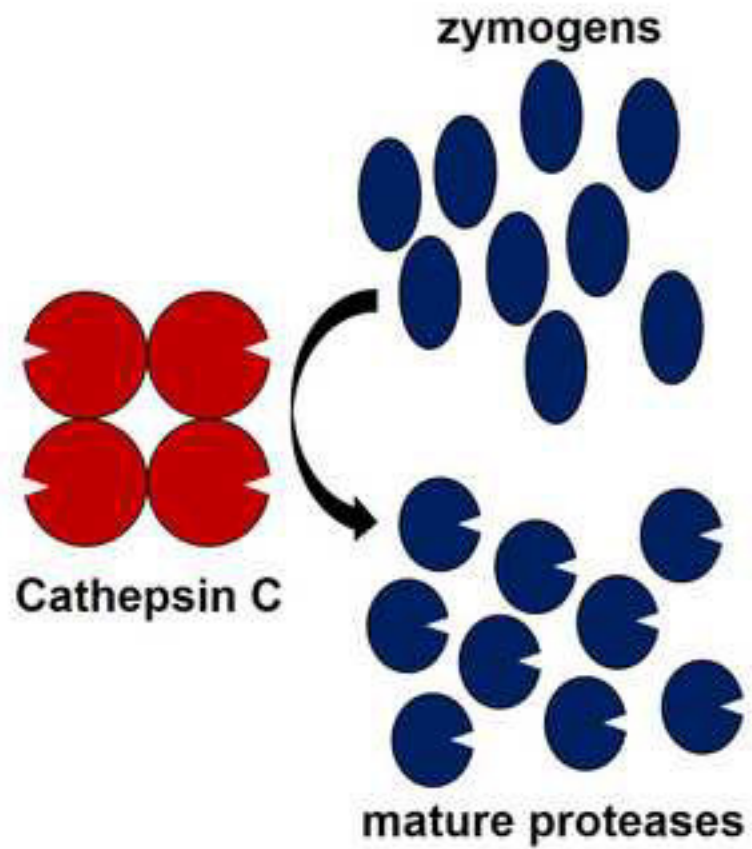












DISEASE

THERAPEUTIC APPROACH

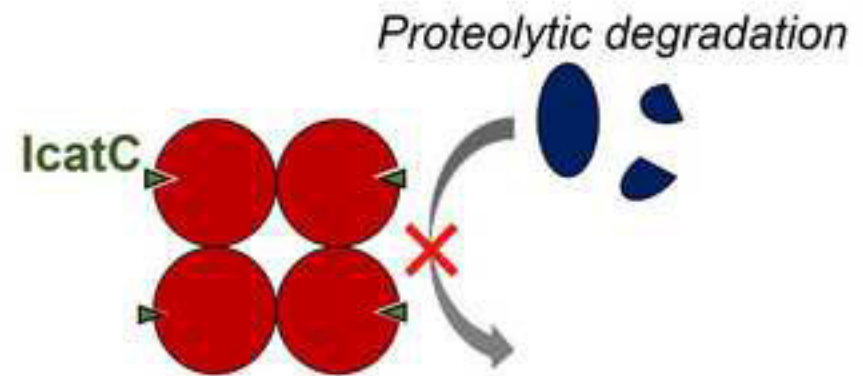


Table I
Potency and selectivity of IcatC on human proteases

	IC ₅₀ (μM)
CatC	0.015 ± 0.001*
CatK	> 30
CatL	> 100
CatS	> 100
CatH	> 100
HNE	> 100
CatG	> 100
PR3	> 100
DPPIV	> 100
Aminopeptidase N	> 100

The inhibitor potencies were determined on recombinant or purified proteases.

* Value is the mean ± S.D. of three separate determinations.